

Strategic approaches to overcome resistance against Gram negative pathogens using #-lactamase inhibitors and #-lactam enhancers: The activity of three novel diazabicyclooctanes, WCK 5153, zidebactam (WCK 5107), and WCK 4234

Krisztina M. Papp-Wallace, Nhu Q. Nguyen, Michael R. Jacobs, Christopher R. Bethel, Melissa D. Barnes, Vijay Kumar, Saralee Bajaksouzian, Susan D. Rudin, Philip N. Rather, Satish Bhavsar, Tadiparthi Ravikumar, Prasad K. Deshpande, Vijay Patil, Ravindra Yeole, Sachin S. Bhagwat, Mahesh V. Patel, Focco van den Akker, and Robert A. Bonomo

J. Med. Chem., **Just Accepted Manuscript** • DOI: 10.1021/acs.jmedchem.8b00091 • Publication Date (Web): 07 Apr 2018

Downloaded from <http://pubs.acs.org> on April 7, 2018

Just Accepted

“Just Accepted” manuscripts have been peer-reviewed and accepted for publication. They are posted online prior to technical editing, formatting for publication and author proofing. The American Chemical Society provides “Just Accepted” as a service to the research community to expedite the dissemination of scientific material as soon as possible after acceptance. “Just Accepted” manuscripts appear in full in PDF format accompanied by an HTML abstract. “Just Accepted” manuscripts have been fully peer reviewed, but should not be considered the official version of record. They are citable by the Digital Object Identifier (DOI®). “Just Accepted” is an optional service offered to authors. Therefore, the “Just Accepted” Web site may not include all articles that will be published in the journal. After a manuscript is technically edited and formatted, it will be removed from the “Just Accepted” Web site and published as an ASAP article. Note that technical editing may introduce minor changes to the manuscript text and/or graphics which could affect content, and all legal disclaimers and ethical guidelines that apply to the journal pertain. ACS cannot be held responsible for errors or consequences arising from the use of information contained in these “Just Accepted” manuscripts.

1
2
3
4
5
6
7
8 **Strategic approaches to overcome resistance against Gram negative pathogens**
9
10 **using β -lactamase inhibitors and β -lactam enhancers: The activity of three novel**
11 **diazabicyclooctanes, WCK 5153, zidebactam (WCK 5107), and WCK 4234**
12
13
14
15
16

17 Krisztina M. Papp-Wallace^{1-3,*}, Nhu Q. Nguyen³, Michael R. Jacobs^{2,6}, Christopher R. Bethel¹,
18
19 Melissa D. Barnes^{1,2}, Vijay Kumar³, Saralee Bajaksouzian^{2,6}, Susan D. Rudin^{1,2}, Philip N.
20
21 Rather^{7,8}, Satish Bhavsar⁹, Tadiparthi Ravikumar⁹, Prasad K. Deshpande⁹, Vijay Patil⁹, Ravindra
22
23 Yeole⁹, Sachin S. Bhagwat⁹, Mahesh V. Patel⁹, Focco van den Akker^{3,*}, and Robert A. Bonomo¹⁻
24
25 5,*
26
27
28
29
30

31 ¹Research Service, Louis Stokes Cleveland Department of Veterans Affairs Medical Center, 10701 East
32
33 Boulevard, Cleveland, OH 44106, USA; Departments of ²Medicine, ³Biochemistry, ⁴Pharmacology,
34
35 ⁵Molecular Biology and Microbiology, Case Western Reserve University School of Medicine, Cleveland,
36
37 OH 44106, USA; ⁶Department of Pathology, University Hospitals, Cleveland Medical Center, Cleveland,
38
39 OH 44106, USA; ⁷Department of Microbiology and Immunology, Emory University School of Medicine
40
41 Atlanta, GA 30322, USA; ⁸Research Service, Atlanta VA Medical Center, Decatur, GA 30033; and
42
43 ⁹Wockhardt Research Centre, Aurangabad, India
44
45
46
47
48
49
50
51
52
53
54
55
56
57
58
59
60

Abstract

Limited treatment options exist to combat infections caused by multidrug-resistant (MDR) Gram negative bacteria possessing broad-spectrum β -lactamases. The design of novel β -lactamase inhibitors is of paramount importance. Here, three novel diazabicyclooctanes (DBOs), WCK 5153, zidebactam (WCK 5107), and WCK 4234 (compounds **1-3**) were synthesized and biochemically characterized against clinically important bacteria. Compound **3** inhibited class A, C and D β -lactamases with unprecedented k_2/K values against OXA carbapenemases. Compounds **1** and **2** acylated class A and C β -lactamses rapidly, but not the tested OXAs. Compounds **1-3** formed highly stable acyl-complexes via mass spectrometry. Crystallography revealed that the KPC-2-compounds **1-3** structures adopted a “chair conformation” with the sulfate occupying the carboxylate binding region. The cefepime-**2** and meropenem-**3** combinations were efficacious in murine peritonitis and neutropenic lung infection models using MDR *Acinetobacter baumannii*. Compounds **1-3** are novel β -lactamase inhibitors that demonstrate potent cross-class inhibition and clinical studies targeting MDR infections are warranted.

INTRODUCTION

In February of 2017, carbapenem-resistant Enterobacteriaceae (CRE), *Pseudomonas aeruginosa*, and *Acinetobacter baumannii* were designated as the “top priority pathogens” for the development of novel antibiotics by the World Health Organization¹. The presence of β -lactamases in these Gram negative pathogens is largely responsible for this global threat. Of the serine β -lactamases, *Klebsiella pneumoniae* carbapenemase, KPC, *Pseudomonas*-derived cephalosporinase, PDC, *Acinetobacter*-derived cephalosporinase, ADC, and the carbapenem hydrolyzing class D OXA β -lactamases (e.g., OXA-23, OXA-24/40, and OXA-48) represent the most prevalent and problematic β -lactam inactivating hydrolases. Presently, three strategies are used by the pharmaceutical industry to overcome β -lactamase mediated resistance: *i*) the design of new β -lactams resistant to hydrolysis; *ii*) the synthesis of new β -lactamase inhibitors (BLIs); and *iii*) the development of new antimicrobial classes². An emerging and appealing strategy to overcome diverse mechanisms of β -lactamase mediated resistance deploys an unconventional concept of a β -lactam enhancer (BLE). BLEs represent a new antimicrobial class and work by providing complimentary penicillin binding protein (PBP) inhibition to a partner β -lactam. By targeting two different PBPs, BLEs act synergistically to promote killing of the bacterial cell. The remarkable aspect of the BLE mechanism is that it can operate independently of BLIs.

Currently in the United States, the BLIs available in the clinic are clavulanic acid (approved in 1984), sulbactam (approved in 1986), tazobactam (approved in 1993), avibactam (approved in 2015), and vaborbactam (approved in 2017). During the past 30 years, clavulanic acid, sulbactam, and tazobactam have lost efficacy against inhibitor-resistant TEMs (IRTs) and inhibitor-resistant SHVs (IRSs)². With the exception of tazobactam demonstrating fair activity as an inhibitor against certain class C cephalosporinases (CMY-2, $K_i = 40 \mu\text{M}$)³, these three BLIs

1
2
3 possess poor or no activity against the recently emerged class A carbapenemases (e.g., KPC),
4 class B metallo- β -lactamases (e.g., NDM and VIM), and many class D OXA β -lactamases.
5
6

7
8 Diazabicyclooctanes (DBOs) are a new class of BLIs (“second generation” BLIs) that
9 were developed in the early 2000s². Avibactam, the first DBO introduced into clinical practice,
10 inhibits class A carbapenemases, KPC, as well as class C β -lactamases, AmpCs, and when
11 combined with ceftazidime has the ability to target many drug-resistant Enterobacteriaceae^{2, 4-8}.
12 Avibactam, however, possesses limited activity towards class D OXA β -lactamases^{4, 9}.
13 Avibactam is slow to acylate OXA-type β -lactamases with low k_2/K values in the range of 10^1 to
14 $10^3 \text{ M}^{-1}\text{s}^{-1}$. In contrast, avibactam acylates class A and class C β -lactamases in the range of 10^3 -
15 $10^6 \text{ M}^{-1}\text{s}^{-1}$. The recently described atomic structures of OXA-24/40 and OXA-48 revealed that
16 the binding pocket especially where the R¹ side chain of avibactam resides in class D β -
17 lactamases is more hydrophobic with fewer polar residues present, thus potentially affecting
18 binding and acylation of avibactam^{7, 8}.
19
20
21
22
23
24
25
26
27
28
29
30
31
32

33 In the last decade, the DBO class of BLIs expanded to include advanced generation
34 DBOs with modified chemical scaffolds that enhance their activity. The first generation DBO
35 inhibitors, avibactam and relebactam inactivate class A, C, and some class D β -lactamases^{4, 10}.
36 The DBO inhibitors WCK 5153 (compound **1**), zidebactam, formerly WCK 5107 (compound **2**),
37 nacubactam, FPI-1465, and ETX2514 are “dual action inhibitors” as they inhibit PBPs and
38 certain β -lactamases as well as possessing BLE activity^{8, 11-13}. Compound **1** and **2** were shown to
39 be potent inactivators of *P. aeruginosa* PBP-2 and *A. baumannii* PBP-2 resulting in enhanced
40 killing of bacteria when combined with a β -lactam partner¹¹.
41
42
43
44
45
46
47
48
49
50

51 Two challenges need to be overcome to design BLIs with promising therapeutic potential
52 against class D OXA β -lactamases associated with *Acinetobacter* spp.. The first is to readily
53
54
55
56
57
58
59
60

1
2
3 access the sterically constrained active site of such β -lactamases found in the periplasm and
4 imparting inhibitory activity. The second is to effectively traverse the outer membrane and
5 periplasmic space embedded with diverse efflux pumps. Newer generations of BLIs such as
6 avibactam, relebactam and vaborbactam are devoid of activity against class D OXA β -
7 lactamases, which illustrates the challenge in designing such compounds. Sulbactam, which is an
8 “older” or legacy BLI, effectively permeates the outer membrane and reaches the periplasmic
9 compartment of *Acinetobacter*. However, sulbactam fails to inhibit class D OXA β -lactamases,
10 additional evidence of formidable scientific intricacy of the field. This challenge led us to
11 explore the effects of introduction of a nitrile functional group onto the DBO core. Unlike
12 avibactam and relebactam, WCK 4234 (compound **3**), possessing a nitrile side chain (R^1), at the
13 C2 position of the DBO (**Figure 1**), demonstrates expanded activity against class D OXA β -
14 lactamases, including OXA-23 and OXA-51 expressed in *A. baumannii*, while maintaining
15 activity against class A and C β -lactamases¹⁴.
16
17
18
19
20
21
22
23
24
25
26
27
28
29
30
31
32

33 The structure activity relationships (SAR) that prompted the design of compounds **1-3** are
34 presented herein. Furthermore, we evaluate **1**, **2**, **3**, and two DBO comparators, avibactam and
35 relebactam (**Figure 1**, chemical structures) to gain mechanistic insights into their inhibitory
36 activity against representative serine class A, C, and D β -lactamases using steady-state kinetics
37 and mass spectrometry. As a result of these studies, KPC-2 and OXA-24 were chosen for X-ray
38 crystallography analysis to define on an atomic level, the nature of the inactivation mechanism.
39 Finally, the abilities of cefepime-**2** (WCK 5222) and meropenem-**3** (WCK 5999) combinations
40 were evaluated in susceptibility studies and mouse models of infection. Our data show that
41 cefepime-**2** and meropenem-**3** offer promise against pathogens possessing β -lactamases from
42 multiple classes. Notably, the cefepime-**2** combination has completed two Phase I clinical trials
43
44
45
46
47
48
49
50
51
52
53
54
55
56
57
58
59
60

1
2
3 (NCT02707107; NCT02532140) and another Phase I clinical trial is actively recruiting
4 participants (NCT02942810).
5
6
7
8
9

10 RESULTS AND DISCUSSION

11
12 **Synthesis of a Novel Class of DBOs.** Starting with a DBO scaffold, a pathway to identify
13 compounds with activity against Gram-negative PBP-2 and β -lactamases led to the evolution of
14 this novel bicyclo hydrazide (BCH) series¹¹. The key medicinal chemistry challenge involved
15 identifying a side chain (R^1) at the C-2 position of the DBO core that was able to penetrate the
16 periplasmic space of Gram negative bacteria and access PBP targets on the cytoplasmic
17 membrane. After developing SAR with linear-chain and cyclic-amines¹⁵, a cyclic secondary
18 amine was employed on the acyl hydrazide to obtain compounds with high affinity binding for
19 the PBP-2 of *Enterobacteriaceae*, *P. aeruginosa* and *A. baumannii*¹¹. Thus, the hydrazide as a R^1
20 side chain bearing a free amine at the appropriate length from the C-2 position of DBO core was
21 found to be essential for antibacterial potency. Enhancement of antibacterial activity was further
22 achieved by chiral separation of the isomers of the racemic secondary cyclic amine. SAR
23 generated the lead compounds **1**¹⁶ and **2**¹⁷ and bearing pyrrolidine and piperidine side chains,
24 respectively (**Figure 2A**). These compounds demonstrated targeted antibacterial profile
25 encompassing *Enterobacteriaceae* and non-fermenter organisms¹¹.
26
27
28
29
30
31
32
33
34
35
36
37
38
39
40
41
42
43
44

45 To obtain a DBO that demonstrates expanded antimicrobial activity against *A. baumannii*
46 producing class D carbapenemases, OXA-23 and OXA-51, while maintaining activity in Gram
47 negatives producing class A and C β -lactamases¹⁴, we next examined the properties of nitrile
48 group in the literature¹⁸. Since nitrile bonds are polarized, they act as hydrogen acceptors and
49 form hydrogen bonds with amino acids and water and thus can bind to a protein backbone.
50
51
52
53
54
55
56
57
58
59
60

1
2
3 Furthermore, the strong dipolar nature of the nitrile permits it to act as a hydroxyl or carboxyl
4 bioisostere. The introduction of nitrile additionally reduces the clogP of the molecule thereby
5 reducing its lipophilicity and thus improving the chances of penetration of the porin channels in
6 Gram-negative organisms. The nitrile group is not readily metabolized, which could be
7 advantageous. Importantly, the nitrile reduces the steric bulk of the R¹ substituent of DBOs
8 such as avibactam and thus could yield a better fit into sterically-constrained active sites, such as
9 the class D OXA β -lactamase's active site. Based on our observations, we replaced the amide
10 functionality of avibactam with a nitrile, generating compound **3** (Figure 2B).
11
12
13
14
15
16
17
18
19
20
21
22

23 **Compound 3 is a Highly Potent Inactivator of Class A, C, and D β -Lactamases.** Compound
24 **3** inhibited all β -lactamases tested with $K_{i\text{ app}}$ values ranging from 0.1 to $\leq 8\ \mu\text{M}$ (Table 1).
25 Testing KPC-2, **3** possessed the highest acylation rate (k_2/K value) by nearly 9-fold compared to
26 relebactam. Additionally, **3** was the only DBO capable of acylating OXA-23, OXA-24/40, and
27 OXA-48. The highest k_2/K value obtained was with OXA-48 and **3**, $6.4 \pm 0.6 \times 10^5\ \text{M}^{-1}\text{s}^{-1}$.
28
29
30
31
32
33
34

35 The rate (k_{off}) at which the DBOs deacylate (recyclize) the β -lactamases to re-form active
36 DBO was also determined (Table 1). The rank order of **3** recyclization after inhibition was as
37 follows: PDC-3 \gggg ADC-7 $>$ OXA-48 $>$ OXA-23 $>$ OXA-24/40 $>$ KPC-2. After **3** inhibition,
38 PDC-3 recovered the ability to hydrolyze nitrocefin the fastest.
39
40
41
42
43

44 The k_{off} values correspond to the residence time half-lives as listed in Table 1.
45 Comparing all of the k_{off} values, avibactam was the DBO with the lowest k_{off} values. The β -
46 lactamases/DBO combination with the longest residence time half-life was OXA-24/40 and
47 avibactam at $1,823\ \text{min}^{19}$. The turnover number ($k_{\text{cat}}/k_{\text{inact}} = t_n$) at 24 hours or the number of
48 inhibitor molecules hydrolyzed before the β -lactamase is inactivated was also measured (Table
49 **1**). KPC-2 possessed a $k_{\text{cat}}/k_{\text{inact}}$ value of 1 for all the DBOs tested. In contrast, ADC-7
50
51
52
53
54
55
56
57
58
59
60

1
2
3 demonstrated turnover of all of the DBOs; the $t_n = 6$ at 24 hr. Although insignificant in terms of
4 the bacterial cell cycle, the basis for this catalytic ability is being investigated. To put relative t_n
5 values into context, the t_n of KPC-2 for clavulanic acid is 2,500 at 15 min with KPC-2 being
6 resistant to inhibition by clavulanic acid²⁰.
7
8
9
10
11
12
13

14 **Compounds 1 and 2 are Potent Inhibitors of Representative AmpC β -Lactamases.**

15 Compounds **1** and **2** possessed 3-8 fold and 18-25-fold lower $K_{i\text{ app}}$ values against ADC-7 and
16 PDC-3, respectively compared to avibactam and relebactam (**Table 1**). Against ADC-7 and
17 PDC-3, the highest acylation rates ($3.1 \pm 0.3 \times 10^4 \text{ M}^{-1}\text{s}^{-1}$ - $6.3 \pm 0.6 \times 10^5 \text{ M}^{-1}\text{s}^{-1}$) were for **1** and
18
19
20
21
22
23
24 **2**.

25
26
27
28 **1, 2, and 3 Form Highly Stable Complexes with Class A, C, and D β -Lactamases.** Upon
29 formation of the acyl-enzyme complex between avibactam and KPC-2, avibactam was shown to
30 desulfate (E-I*) and eventually deacylate from KPC-2 (**Figure 3A and 3B**)⁴. To determine the
31 intermediates in the reaction pathway between β -lactamase-DBO complexes in this study, we
32 performed timed mass spectrometry with β -lactamases that were incubated with the DBOs at an
33 equimolar ratio for 5 min and 24 hr.
34
35
36
37
38
39
40
41

42 Analyzing the reaction intermediates between KPC-2 and either **1** ($+378 \pm 5$ amu), **2**
43 ($+392 \pm 5$ amu), **3** ($+247 \pm 5$ amu) or relebactam ($+349 \pm 5$ amu), formed adducts, did not
44 undergo a secondary chemical reaction; notably, desulfation was also not observed (**Table 2**).
45 However with avibactam, loss of the sulfate (-97 ± 5 amu) was demonstrated with KPC-2 after a
46 24 hr incubation. For ADC-7, the full adducts were detected with all DBOs, except a minor loss
47 of the sulfate (-80 ± 5 amu) was detected with **3** and avibactam at both 5 min and 24 hr (**Table**
48
49
50
51
52
53
54
55
56
57
58
59
60

1
2
3 **2)**. Moreover, hydrolysis of **1**, **2**, **3**, and avibactam occurred as apo-ADC-7 ($40,639 \pm 5$ amu) was
4 noted; only relebactam was not hydrolyzed under these conditions. These data are consistent
5
6 with the $k_{\text{cat}}/k_{\text{inact}}$ values obtained for ADC-7 at 24 hr (**Table 1**).
7
8

9
10 During protein purification, two isoforms ($40,654 \pm 5$ amu and $40,785 \pm 5$ amu) of the
11 PDC-3 β -lactamase were detected. We attribute this finding to a “ragged” N-terminus (different
12 amino acids at N-terminus) that occurs when proteins are overexpressed. As with the ADC-7 β -
13 lactamase, a minor loss of the sulfate side chain (-80 ± 5 amu) was observed with PDC-3 β -
14 lactamase after incubation with **3** and avibactam at both 5 min and 24 hr. When the OXA-23,
15 OXA-24/40, or OXA-48 β -lactamases were incubated with **3**, three peaks were obtained, the
16 major peak identified was the full adduct ($+246 \pm 5$ amu), while two minor peaks corresponding
17 to apo-enzyme and the enzyme-DBO complex minus the sulfate ($+166 \pm 5$ amu) at both 5 min
18 and 24 hrs. In the reaction of OXA-48 β -lactamase with avibactam, only the loss of the sulfate
19 (-80 ± 5 amu) was distinguished at 5 min. At 24 hr, the full avibactam adduct ($+265 \pm 5$ amu)
20 was observed with the OXA-48 β -lactamase.
21
22
23
24
25
26
27
28
29
30
31
32
33
34
35

36 Interestingly, different mass adducts were discerned, a -80 amu with **3** and avibactam
37 with the class C and D β -lactamases and -97 amu adduct with avibactam and KPC-2 (**Figure**
38 **3B**). **3** undergoes a different desulfation mechanism (reaction) compared to the one observed
39 with avibactam and KPC-2 as a -80 amu peak is detected corresponding to hydrolytic loss of
40 SO_3 , which is speculated to result in the hydroxylamine. The significance of this finding is being
41 further explored.
42
43
44
45
46
47
48
49
50
51

52 **Interactions of 1, 2, and 3 with β -Lactamases are Reversible.** To confirm the reversibility of
53 **1**, **2**, and **3**, an acyl-transfer experiment was conducted using KPC-2 as the donor β -lactamase
54
55
56
57
58
59
60

1
2
3 and TEM-1 as the recipient β -lactamase. The donor β -lactamase was pre-incubated with the
4 DBO at equimolar ratio. Then, the recipient β -lactamase was added to the reaction and at 15 sec
5 and 5 min, the reactions were terminated and ESI-MS was conducted. Avibactam was
6 previously shown to transfer slowly from TEM-1 to CTX-M-15 with a minor CTX-M-15-
7 avibactam population observed at 2 min⁵. The maximum transfer of avibactam from TEM-1 to
8 CTX-M-15 was observed at 30 min. Here, after complete inactivation (1 min incubation time)
9 by a equimolar ratio of KPC-2 to compounds **1**, **2**, or **3** was obtained, then equimolar amount of
10 TEM-1 was added and the reactions were terminated by at the addition 1% acetonitrile and 0.1%
11 formic acid. The mass spectrometry results implied that **1**, **2**, and **3** are reversible (**Figure 3C**).
12 Within 15 sec, **3** transferred to TEM-1, while for **1** and **2**, 5 min was required. **1**, **2**, and **3**
13 transfer faster than avibactam, which directly correlates to the k_{off} values observed (**Table 1**).
14
15
16
17
18
19
20
21
22
23
24
25
26
27
28
29
30

31 **KPC-2 β -Lactamase Crystal Structures with **1**, **2**, and **3**.** The crystal structures of the DBO
32 inhibitors, **1**, **2**, and **3** bound to KPC-2 were obtained via soaking experiments and using co-
33 crystallization (**Figure 4**, **Figure S1**, and **Table S1**). The inhibitors were refined with 100%
34 occupancy yielding low B-factors for the inhibitors (**Table S1**); this indicates full occupancy of
35 the inhibitors in agreement with the appearance of strong inhibitor electron density. With each
36 complex structure determined via these two methods, unexpected differences were obtained for
37 the **1** and **2** structures: we observed desulfation of these two DBO inhibitors when co-
38 crystallized, but not when soaked into the KPC-2 crystals (**Figure S1**); these differences were
39 not observed for **3**. Desulfation of a similar DBO, avibactam, by KPC-2 was previously also seen
40 and found to be a slow process²¹. We subsequently probed the KPC-2-mediated desulfation of
41 these two DBOs using mass spectrometry and also observed this phenomenon at lower pH values
42
43
44
45
46
47
48
49
50
51
52
53
54
55
56
57
58
59
60

1
2
3 similar to the pH of the crystallization condition (**Figure S1**). Due to the non-physiological pH
4 and slow rate of this reaction, our discussion will therefore focus on the structures obtained by
5 soaking.
6
7
8
9

10 The three DBO inhibitors adopt a similar conformation when bound covalently to S70 in
11 the active site of KPC-2. The 6-membered ring of the DBO adopts a chair conformation with the
12 sulfate moiety occupying the carboxylate binding pocket of the active site. The sulfate moiety in
13 **3** was observed to be in two conformations (**Figure 4B**), whereas this moiety in the other two
14 DBOs adopted a single conformation. In all three structures, the sulfate makes hydrogen bonds
15 with T235, T237, S130, and is positioned about 4.5 Å from R220. The carbonyl oxygen in each
16 of the three DBO complexes is located in the oxyanion hole formed by the backbone nitrogens of
17 S70 and T237. The R-group moieties that distinguish the inhibitors from each other make
18 different interactions with KPC-2. The R-group nitrile moiety in **3** makes a hydrogen bond with
19 N132 whereas the R-groups in **1** and **2** make interactions with N132, the deacylation water
20 (W#1), and some additional interactions with other water molecules (**Figure 4B**). The R-group
21 in **2** also makes a hydrogen bond with the backbone oxygen of C238; this interaction is not
22 observed in the avibactam:KPC-2 complex²² nor in the relebactam:AmpC complex¹⁰.
23
24
25
26
27
28
29
30
31
32
33
34
35
36
37
38
39

40 The three DBO inhibitor structures are all in a very similar position and orientation as
41 shown by super-positioning (**Figure 5**). These positions and orientations are very similar to that
42 of avibactam bound to KPC-2; the ring structures of these DBOs all adopt the chair conformation
43 (**Figure 5**). The KPC-2 protein in the DBO complexes also adopts a similar conformation except
44 for residue W105 for which there is considerable conformational variability compounded by
45 some structures even having two alternative conformations for this residue (**Figure 5**). We show
46 molecule B of the **3**:KPC-2 complex in the superpositioning to further illustrate this point
47
48
49
50
51
52
53
54
55
56
57
58
59
60

1
2
3 **(Figure 5)**. The superpositioning also revealed a subtle clustering of the DBO ring positions with
4
5 **1** and **2** in one cluster, the **3** molecule A and B in a second cluster, and avibactam in a third
6
7 slightly different orientation **(Figure 5)**. These differences are likely due to the different R-
8
9 group substituents.
10

11
12
13
14 **OXA-24/40-Compound 3 Crystal Structure.** We next analyzed a structure of **3** bound to the
15
16 OXA-24/40 β -lactamase **(Figure 6A and 6B)**. Overall, **3** binds to the OXA-24/40 β -lactamase in
17
18 a similar fashion to when bound to KPC-2 except for a few changes mostly due to differences
19
20 between the protein. **3** is covalently bound to the catalytic S81 residue. The **3**'s sulfate moiety is
21
22 interacting with R261, S219, K218, and S128. The carbonyl oxygen atom is situated in the
23
24 oxyanion hole, as in KPC-2. Unlike KPC-2, the nitrile moiety of **3** is not directly interacting with
25
26 the protein.
27
28
29

30
31 In the **3**-OXA-24/40 β -lactamase complex, we do not observe carboxylation of K84 as
32
33 was observed in OXA-24/40 complexes bound to either penicillanic acid sulfones²³ or boronic
34
35 acid inhibitors²⁴. Instead, this position is filled by the presence of a chloride ion observed in two
36
37 alternate positions with occupancies of 0.63 and 0.37 (labeled Cl1 and Cl2, respectively, in
38
39 **Figure 6C)**. This chloride ion is present due to the HCl used to pH the cacodylate buffer.
40
41 Superpositioning of the **3**:OXA-24/40 structure with that of the avibactam:OXA-24/40
42
43 complex²⁵ indicates that avibactam and **3** have a very similar binding mode including a chair
44
45 conformation of the DBO ring. The DBO inhibitors sit on the inner side of the active site bridge
46
47 formed by residues M223 and Y112. The avibactam:OXA-24/40 complex neither has a
48
49 carboxylated K84 nor does not it have a chloride ion bound; instead it has CO₂ bound at this
50
51 position **(Figure 6C)**. It is interesting to note that the class D OXA β -lactamases were found to
52
53
54
55
56
57
58
59
60

1
2
3 be inhibited by chloride ions that compete for the carboxylation of K84²⁶ including OXA-
4 24/40²⁷; the biological significance of halide binding, if any, is not yet established for OXA-
5
6 24/40.
7
8
9

10
11
12 **Inhibitory Activity of DBOs against Bacterial Cells.** Compound **3**, avibactam, and relebactam
13 are BLIs. **1** and **2** can also inhibit β -lactamases, but are additionally able to inactivate PBPs and
14 serve as BLEs¹¹. As a result, the DBOs either alone or in combination with either cefepime or
15 meropenem were tested in whole cell assays to obtain minimum inhibitory concentrations
16 (MICs). The panel of isolates selected included a set of isogenic strains expressing a single β -
17 lactamase and clinical isolates of Enterobacteriaceae producing *bla*_{KPC-2} or *bla*_{OXA-48},
18 ceftazidime-avibactam-resistant *P. aeruginosa*, and *A. baumannii* producing *bla*_{OXA-23} and/or
19 *bla*_{OXA-24/40}. These isolates represent some of the most difficult to treat Gram negative pathogens
20 and they produce the most challenging β -lactamases to inhibit.
21
22
23
24
25
26
27
28
29
30
31
32

33 Isogenic *E. coli* DH10B with pBR322-*catI-bla*_{KPC-2} and *A. baumannii* Δ *bla*_{ADC} with
34 pWH1266 *bla*_{OXA-23} or *bla*_{OXA-24} demonstrated MICs of >16 μ g/mL for cefepime and \geq 8 μ g/mL
35 for meropenem (**Table 3**). All MICs of cefepime or meropenem combined with all five DBOs
36 (using fixed concentrations of DBOs of 4 and/or 8 μ g/mL) against *E. coli* DH10B with pBR322-
37 *catI-bla*_{KPC-2} were reduced to \leq 0.12 μ g/mL. Only cefepime combined with **3** restored
38 susceptibility for *A. baumannii* Δ *bla*_{ADC} with pWH1266 *bla*_{OXA-23} (MIC = 2 μ g/mL). *A.*
39 *baumannii* Δ *bla*_{ADC} with pWH1266 *bla*_{OXA-24/40} was resistant to all combinations tested.
40
41
42
43
44
45
46
47
48

49 A panel of clinical isolates of *Klebsiella pneumoniae* that carry either *bla*_{KPC-2} or *bla*_{KPC-3}
50 including colistin susceptible (ColS) and colistin resistant (ColR) strains and other
51 Enterobacteriaceae expressing *bla*_{KPC} were also tested. **1**, **2**, **3**, avibactam, and relebactam
52
53
54
55
56
57
58
59
60

1
2
3 restored susceptibility to cefepime and meropenem in all isolates (**Table 3**). Thus for KPC
4 expressing strains, both cefepime and meropenem in combination with **3** provided comparable
5 activity.
6
7
8
9

10 The DBOs were tested against a panel of clinical isolates of Enterobacteriaceae that
11 expressed *bla*_{OXA-48} or *bla*_{OXA-48} mutants (**Table 3**). **1**, **2**, **3**, and avibactam restored susceptibility
12 to cefepime and meropenem in all isolates tested even though **1** and **2** lack inhibition of OXA-48.
13 Presumably, the **1** and **2** effect is the result of PBP inhibition and their BLE property.
14 Combinations with relebactam were less effective. Overall, Enterobacteriaceae expressing
15 *bla*_{OXA-48} family members were more susceptible in combinations with meropenem than with
16 cefepime.
17
18
19
20
21
22
23
24
25

26 Five clinical strains of *P. aeruginosa* from an archived collection previously found to be
27 resistant to ceftazidime-avibactam were also tested²⁸. Combination of cefepime and **1** or **2** at 8
28 $\mu\text{g/mL}$ restored cefepime susceptibility (MICs $\leq 0.12\text{-}0.5 \mu\text{g/mL}$) to some of these highly drug
29 resistant strains (**Table 3**). PBP-2 inhibition and BLE activity of **1** and **2** most likely provided
30 this advantage against *P. aeruginosa*¹¹.
31
32
33
34
35
36
37

38 The DBOs were tested against a panel of clinical isolates of *A. baumannii* that possess
39 either *bla*_{OXA-23} or *bla*_{OXA-24/40} or both *bla*_{OXA-23} and *bla*_{OXA-24/40} (**Table 3**). Compounds **1**, **2**, and
40 **3** demonstrated some activity against these strains when combined with cefepime. However,
41 against dual OXA-carbapenemases expressing strains, most combinations showed high MICs.
42 Given that **3** is a potent inhibitor of OXA-23 and OXA-24/40, limited penetration of cefepime
43 and/or **3** is a possible cause for lack of efficacy in these strains. Overall, the meropenem-**3**
44 combination was more active against *A. baumannii* with *bla*_{OXA-23} and/or *bla*_{OXA-24/40}, which is in
45 agreement with another study¹⁴.
46
47
48
49
50
51
52
53
54
55
56
57
58
59
60

To determine that cause of the higher MICs for the β -lactam-DBO combinations against *A. baumannii*, *A. baumannii* ATCC 17978 was used as the parent strain and different efflux pump components were knocked-out as well as *blhA*, (β -lactam hyper susceptibility), which is a determinant of intrinsic β -lactam resistance and is also involved in cell division. AdeABC, AdeFGH, AdeIJK, and AcrA systems are the major Resistance-Nodulation-Division (RND) efflux systems in *Acinetobacter*. These systems are three-component efflux pumps where AdeA, AdeF, AdeI, AcrA are the membrane fusion protein (MFP), AdeB, AdeG, and AdeJ are the multidrug transporter and AdeC, AdeI, and AdeK are the outer membrane protein (OMP). AcrR is the transcriptional regulator of the AcrA RND efflux pump. The AdeB and AdeJ efflux pump components may have some contribution to cefepime efflux as when the corresponding genes were deleted, susceptibility was increased (**Table S2**). Overall, the strains were all susceptible to single agents as well as the combinations.

Cefepime-Compound 2 and Meropenem-Compound 3 was Tested against MDR *A. baumannii* in Murine Models of Peritonitis and Neutropenic Lung Infection. The protective doses (PD₅₀ and PD₉₀) or the dose of antibiotic that protects 50% or 90% of the infected mice was determined for cefepime-**2** and meropenem-**3** using a murine peritonitis model. Mice were intraperitoneally infected with one of three different *A. baumannii* strains (NCTC 13301 carrying *bla*_{OXA-23} and *bla*_{OXA-51-like}, NCTC 13303 possessing *bla*_{OXA-26} (*bla*_{OXA-24/40-like}) and *bla*_{OXA-51-like}, and SL46 with *bla*_{OXA-23} and *bla*_{OXA-51}); MICs are presented in **Table 4**. The mice were treated with either cefepime, cefepime-**2**, meropenem, meropenem-**3**, tigecycline, or colistin and survival patterns were monitored for 7 days. The PD_{50/90} for cefepime-**2** ranged between 50-100 mg/kg for cefepime and 23.23-52.30 mg/kg for **2** (**Table 4**). Remarkably, the cefepime-**2** PD_{50/90}

1
2
3 provide just 25% exposure compared to the exposures at the selected clinical dose^{29, 30}. For
4 meropenem-**3**, the PD_{50/90} were meropenem: 25-50 mg/kg and **3**: 16.30-66.17 mg/kg (**Table 4**).
5
6 Tigecycline, although employed at supra-therapeutic doses (6.25 mg/kg administered as two
7
8 doses) failed to protect infected mice (**Table 4**). Considering the colistin MIC values of 0.5-1
9
10 µg/mL, colistin appropriately exhibited low PD_{50/90} values (**Table 4**)³¹.
11
12
13

14
15 To determine the *in vivo* eradication efficacy of cefepime-**2** and meropenem-**3**, a
16
17 neutropenic lung infection model was used in which mice were intranasally infected with a
18
19 clinical isolate of *A. baumannii* SL04 carrying *bla*_{OXA-23} and *bla*_{OXA-51}. The MICs for this isolate
20
21 are as follows: cefepime: 256 µg/mL, **2**: ≥512 µg/mL, cefepime-**2**: 32 µg/mL, imipenem: 64
22
23 µg/mL, meropenem: 64 µg/mL, meropenem-**3**: 8 µg/mL, colistin: 2 µg/mL, and tigecycline: 4
24
25 µg/mL. Thus, the MIC of cefepime was reduced by 8-fold when in combination with **2**. Two
26
27 hours post infection, mice were treated by q2h dosing for 24 h by a subcutaneous route. Three
28
29 hours post last dose (i.e. 27 h post infection), the murine lungs were removed and colony
30
31 forming units (CFUs) were determined. Treatment of infected mice with cefepime (50 mg/kg),
32
33 meropenem:cilastatin (25-25 mg/kg), and imipenem:cilastatin (25-25 mg/kg) revealed a 0.67-
34
35 1.31 log increase in bacterial burden as compared to the 2 h count (**Figure 7A**). Treatment
36
37 with cefepime-**2** (50-8.33 mg/kg) resulted in a 3 log kill (**Figure 7B**). Notably, the addition of **2**
38
39 to cefepime enhanced the bactericidal action of cefepime even at very low dose of 50 mg/kg³².
40
41 Similarly, the addition of **3** at 4.68 mg/kg, to meropenem:cilastatin (25-25 mg/kg) resulted in a
42
43 2.47 log kill (**Figure 7B**). Conversely, relebactam at 18.75 mg/kg combined with
44
45 imipenem:cilastatin at 25 mg/kg resulted in a 0.86 log increase in CFUs (**Figure 7B**). It is
46
47 important to note that *A. baumannii* NCTC 13301, SL 46 and SL04 produce OXA-23 and OXA-
48
49 51, which are not inhibited by **2**. Even with higher MICs, the cefepime-**2** combination provided
50
51
52
53
54
55
56
57
58
59
60

1
2
3 potent *in vivo* efficacy against these strains based on its BLE mechanism of action³³. The most
4 significant feature of the BLE mechanism is the augmentation of the pharmacodynamic action
5 of the partner β -lactam antibiotic. In addition, BLEs enhance the arsenal of agents required to
6 overcome β -lactamases. A further challenge in designing novel BLIs also stems in imparting
7 them with structural features which facilitate their efficient penetration into MDR Gram negative
8 pathogens. Many contemporary MDR pathogens express efflux pumps as well as mutations in
9 the genes encoding various outer membrane proteins. These mechanisms could impact the
10 uptake of some newer BLIs that show potent activity against inhibitor resistant enzymes. **3** by
11 virtue of its potent BLI activity for OXA-carbapenemases and ease of penetration restores the
12 efficacy of meropenem against MDR *A. baumannii*³¹.
13
14
15
16
17
18
19
20
21
22
23
24
25
26
27

28 CONCLUSIONS

29
30 Here, we revealed the biochemical activity of three novel DBOs, compounds **1**, **2**, and **3** against
31 some of the most challenging β -lactamases in Gram negative bacteria (i.e., KPC-2, PDC-3,
32 ADC-7, OXA-23, OXA-24/40, and OXA-48). We also verified *in vivo* efficacy of cefepime-**2**
33 and meropenem-**3**. **3** was found to extend the kinetic inhibitory profile of DBOs to OXA
34 carbapenemases, while maintaining class A and C activity. **1** and **2** demonstrated increased
35 potency against class C β -lactamases compared to avibactam and relebactam. **1** and **2** are unique
36 DBOs in that they also target PBPs of many Gram negative pathogens and have BLE activity.
37 Thus, they work synergistically when paired with an appropriate β -lactam antibiotic and
38 overcome β -lactamase mediated resistance without the need to inhibit multiple β -lactamases.
39 The addition of compounds **1**, **2**, and **3** to our armamentarium would be highly beneficial as the
40 clinically available β -lactams and β -lactam-BLI combinations are not effective against these
41
42
43
44
45
46
47
48
49
50
51
52
53
54
55
56
57
58
59
60

1
2
3 refractory Gram negative pathogens. Finally, compounds **1**, **2**, and **3** exemplify two divergent
4 strategies in rejuvenating β -lactam antibiotics.
5
6
7
8
9

10 EXPERIMENTAL SECTION

11
12 **Compound Characterization.** Nuclear magnetic resonance spectra were recorded on Mercury
13 400 MHz (Varian Inc.) or 500 MHz (Bruker). The mass spectra were recorded on TQD mass
14 spectrometer (Waters Corp.) using the electrospray ionization technique. Elemental analysis was
15 conducted on Vario-Micro cube elemental analyser (Elementar). Water content was determined
16 using Karl-fisher titration method. The purity (>95%) of all the compounds was established by
17 using high pressure liquid chromatography method with 5 μ m particle size C18 columns (Bonna
18 Agela Technologies for **2** and YMC Technologies for remaining compounds) maintaining
19 solution at 10°C.
20
21
22
23
24
25
26
27
28
29
30
31
32

33 **Synthesis of 1 and 2.** Figure 2A represents construction of BCH backbone intermediate **1b** and
34 **2b**, as a result of coupling of corresponding chiral acid hydrazide **1a** or **2a** with sodium salt of
35 DBO nucleus represented by **A**, by using EDC.HCl as a coupling agent in water (~87% n = 1 and
36 2). Subsequent catalytic hydrogenation (10% Pd/C catalyst) furnished hydroxyl intermediate (**1c**,
37 n = 1 or **2c**, n = 2), in quantitative yield which was subjected to sulfonation reaction immediately
38 by using sulfurtrioxide pyridine complex to afford sulfonated intermediate. Sulfonated
39 intermediate was isolated in the form of tetrabutylammonium salt **1d** (60%, n = 1) or **2d** (87% n
40 = 2). Finally, removal of N-Boc group and tetrabutyl ammonium salt was achieved in one step
41 using excess TFA at 0 to 5°C. Compounds were purified by crystallizing in aqueous iso-propanol
42 to furnish **1 (1e, n = 1, 60%,)**, or **2 (2e, n = 2, 80%)**.
43
44
45
46
47
48
49
50
51
52
53
54
55
56
57
58
59
60

1
2
3 **Synthesis of 3.** Figure 2B represents the synthesis of **3**³⁴, where the sodium salt of DBO core
4 (A) was converted into the mixed anhydride by first treating the sodium salt with triethylamine
5 hydrochloride in dichloromethane and reacting the resulting compound with pivaloyl chloride in
6 presence of a base triethylamine at 0-5 °C, to obtain the mixed anhydride which was as such
7 reacted with a 25% aqueous solution of ammonia in water at -20°C, obtain the amide (**3a**) as off-
8 white solid after workup and purification. The amide (**3a**) was dehydrated with trifluoroacetic
9 anhydride in the presence of triethylamine in dichloromethane at -5°C to RT, to obtain the cyano
10 compound (**3b**). The cyano compound (**3b**) was de-benzylated with 10% Pd/C (50% wet), in a
11 1: 1 (v/v) mixture of DMF: DCM (v/v) under hydrogen atmosphere (50 to 55 psi) to obtain the
12 hydroxyl compound (**3c**) which was immediately sulphated with DMF:SO₃ complex to obtain
13 the sulphate which was isolated as its tetrabutylammonium salt (**3d**) by reacting with
14 tetrabutylammonium acetate. The tetrabutylammonium salt (**3d**) was converted into **3** by passing
15 the salt through a column filled with Indion 225 sodium resin. **3** was obtained as a white solid by
16 lyophilization of the aqueous solution and re-crystallization of the dry powder from a mixture
17 of isopropanol:water.
18
19
20
21
22
23
24
25
26
27
28
29
30
31
32
33
34
35
36
37
38
39

40 **Synthesis of (2S, 5R)-6-sulfoxy-7-oxo-2-(((3R)-pyrrolidine-3-carbonyl)-**
41 **hydrazinocarbonyl]-1,6-diaza-bicyclo[3.2.1]octane, 1 (1e)-** Step-1: (2S, 5R)- 6-benzyloxy-7-
42 oxo-2-(((3R)-N-Boc-pyrrolidine-3-carbonyl)-hydrazino carbonyl]-1,6-diaza-bicyclo[3.2.1]octane
43 (**1b**): Analysis of analytical sample: White solid, 95 gm, 88%; ¹H NMR (CDCl₃): δ 8.61 (br s,
44 1H), 8.21 (br d, 1H), 7.36-7.43 (m, 5H), 5.04 (d, *J* = 11.2Hz, 1H), 4.90 (d, *J* = 11.6 Hz, 1H), 3.99
45 (d, *J* = 6.8 Hz, 1H), 3.60-3.70 (m, 1H), 3.48-3.52 (m, 2H), 3.24-3.40 (m, 2H), 3.04-3.18 (m, 2H),
46 2.98 (t, *J* = 11.6 Hz, 1H), 2.24-2.34 (m, 1H), 2.12 (br s, 2H), 1.91-2.04 (m, 2H), 1.58-1.66 (m,
47
48
49
50
51
52
53
54
55
56
57
58
59
60

1
2
3 1H), 1.43 (s, 9H); Mass: (M-1) = 486.3 for C₂₄H₃₃N₅O₆, HPLC purity: 98.89%. Step-2: (2S, 5R)-
4 6-hydroxy-7-oxo-2-(((3R)-N-Boc-pyrrolidine-3-carbonyl)-hydrazinocarbonyl]-1,6-diaza-
5
6 bicyclo[3.2.1] oct-ane (**1c**): Analysis of analytical sample: White solid, 72 gm, quantitative. ¹H
7
8 NMR (400 MHz, DMSO-d₆): δ 9.70-9.90 (m, 3H), 3.76 (d, *J* = 7.6 Hz, 1H), 3.59 (br s, 1H),
9
10 3.41-3.46 (m, 1H), 3.18-3.29 (m, 2H), 3.13-3.17 (m, 2H), 2.96-2.99 (m, 2H), 1.82-2.05 (m, 4H),
11
12 1.71-1.81 (m, 1H), 1.53-1.71 (m, 1H), 1.37 (s, 9H); Mass: (M-1): 396.2 for C₁₇H₂₇N₅O₆. Step-3:
13
14 Tetrabutyl ammonium salt of (2S, 5R)-6-sulfoxy-7-oxo-2-(((3R)-N-Boc-pyrrolidine-3-
15
16 carbonyl)-hydrazino carbonyl]-1,6-diaza-bicyclo[3.2.1]octane (**1d**): Analysis of analytical
17
18 sample: White foamy solid, 106 gm, 87%; ¹H NMR (400 MHz, CDCl₃): δ 8.76 (br s, 1H), 8.60
19
20 (s, 1H), 4.23 (br s, 1H), 3.97 (d, *J* = 8.0 Hz, 1H), 3.58-3.68 (m, 1H), 3.46-3.54 (m, 2H), 3.30-
21
22 3.34 (m, 1H), 3.22-3.27 (m, 9H), 3.08-3.11 (m, 1H), 12.28-2.33 (m, 1H), 2.10-2.17 (m, 5H),
23
24 1.83-1.89 (m, 1H), 1.57-1.71 (m, 9H), 1.36-1.46 (m, 15H), 0.98 (t, 12H); Mass: (M-1): 476.4 as
25
26 a free sulfonic acid C₁₇H₂₆N₅O₉S.N(C₄H₉)₄. Step-4: **1**: (2S, 5R)-6-sulfoxy-7-oxo-2-(((3R)-
27
28 pyrrolidine-3-carbonyl)-hydrazinocarbonyl]-1,6-diaza-bicyclo[3.2.1]octane (**1e**): Analysis of
29
30 analytical sample: White crystalline solid, 33 gm, 60%; ¹H NMR (400 MHz, DMSO-d₆, D₂O
31
32 exchange) : δ 4.03 (br s, 1H), 3.85 (d, *J* = 7.2 Hz, 1H), 3.02-3.39 (m, 7H), 2.17-2.22 (m, 1H),
33
34 1.99-2.06 (m, 2H), 1.87-1.90 (br s, 1H), 1.70-1.76 (m, 1H), 1.60-1.64 (m, 1H); ¹³C NMR (100
35
36 MHz, DMSO-d₆): δ 171.1, 168.9, 166.1, 58.4, 57.7, 47.0, 46.9, 45.3, 40.1, 28.7, 20.6, 18.4; IR
37
38 (cm⁻¹): 3568, 1746, 1709, 1676, 1279, 1234, 1015; Analysis calculated for **1** monohydrate
39
40 C₁₂H₁₉N₅O₇S.H₂O C, 36.42; H, 5.31; N, 17.70. Found: C, 36.75; H, 5.42; N, 17.69; Mass: (M-1):
41
42 376.3 for C₁₂H₁₉N₅O₇S; HPLC purity 98.46%; Column: 5 μm particle size, 25 cm length YMC
43
44 ODS AM C18 column (YMC Technologies); mobile phase: used was buffer (0.1 M ammonium
45
46 dihydrogen phosphate in water) and methanol in gradient mode; detection: 225 nm; column
47
48
49
50
51
52
53
54
55
56
57
58
59
60

1
2
3 temperature: 25°C; flow rate: 0.7 mL/min.; **1** solution was maintained at 10°C. Specific rotation:
4
5 $[\alpha]_D^{25}$: -47.5° (c 0.5, water).
6
7
8
9

10 **Synthesis of (2S, 5R)-6-sulfooxy-7-oxo-2-(((3R)-piperidine-3-carbonyl)-hydrazinocarbonyl)-**

11 **1,6-diaza-bicyclo[3.2.1]octane 2 (2e)-** Step-1: (2S, 5R)- 6-benzyloxy-7-oxo-2-(((3R)-N-Boc-

12 piperidine-3-carbonyl)-hydrazinocarbonyl]-1,6-diaza-bicyclo[3.2.1]octane (**2b**): To a clear

13 solution of sodium (2S, 5R)-7-oxo-6-benzyloxy-1,6-diaza-bicyclo[3.2.1]octane-2-carboxylate

14 (A, 200 gm, 0.67 mol) in water (3.2 L) was added (R)-N-Boc-piperidine-3-carboxylic acid

15 hydrazide [**2a**, prepared by heating R-ethyl-N-Boc-nipecotic acid and hydrazine, Specific

16 rotation: $[\alpha]_D^{25}$ = -53.5° (c 0.5, methanol), HPLC purity: 99%, 171 gm, 0.70 mol]. The resulting

17 suspension was treated with EDC.HCl (193 gm, 1.01 mol), and HOBt (90.6 gm, 0.67 mol) with

18 vigorous stirring at ambient temperature. The resultant precipitation was filtered after 16 h, and

19 the wet cake was suspended in warm water. The suspension was filtered and dried under vacuum

20 at 45°C to furnish coupled intermediate **2b** as a white powder in 270 gm quantity in 87% yield.

21 NMR analyses is shown below and based on the mass, the product was identified as C₂₅H₃₅N₅O₆.

22 Analysis of analytical sample: ¹H NMR (400 MHz, CDCl₃): δ 8.42 (br s, 2H), 7.37-7.43 (m, 5H),

23 5.06 (d, *J* = 12.2 Hz, 1H), 4.91 (d, *J* = 12.2 Hz, 1H), 4.00 (d, *J* = 7.6 Hz, 1H), 3.84 (br s, 1H),

24 3.52-3.76 (m, 1H), 3.40-3.51 (m, 1H), 3.30 (br s, 1H), 3.18 (br d, *J* = 12.0 Hz, 1H), 3.06 (br d, *J*

25 = 12.0 Hz, 1H), 2.43 (m, 1H), 2.29-2.34 (m, 1H), 1.88-2.00 (m, 4H), 1.60-1.77 (m, 4H), 1.44 (s,

26 9H). ¹³C NMR (100 MHz, DMSO-d₆): δ 172.3, 168.6, 167.3, 154.9, 135.4, 129.2, 128.7, 128.5,

27 80.1, 78.2, 59.1, 57.7, 47.7, 45.5, 44.5, 40.8, 28.3, 27.5, 24.0, 20.6. IR (cm⁻¹): 2974, 1751,

28 1670, 1244, 1153, 1024. Analysis calculated for C₂₅H₃₅N₅O₆: C, 59.86; H, 13.96; N, 7.03.

29 Found: C, 60.26; H, 14.20; N, 7.20. Mass: (M+1): 502.3 for C₂₅H₃₅N₅O₆. HPLC purity: 98.4%.

1
2
3 Step-2: (2S,5R)-6-hydroxy-7-oxo-2-(((3R)-N-Boc-piperidine-3-carbonyl)-hydrazino-carbonyl)-
4 1,6-diaza-bicyclo[3.2.1]octane (**2c**): The coupled intermediate **2b** from step-1 (153 gm, 0.305
5 mol) was dissolved in methanol (1.53 L). To this clear solution, was added 10% Pd/C (15.3 gm,
6 50% wet) catalyst. The suspension was purged with hydrogen gas for 3 h at 35°C under stirring.
7 The catalyst was filtered. The filtrate was evaporated under vacuum below 40°C to provide a
8 crude residue. The residue was triturated with hexanes. The solid was filtered to furnish hydroxyl
9 intermediate **2c** in 125 gm quantity as a white solid in quantitative yield. The intermediate was
10 used immediately for the next reaction. Analysis of analytical sample: ¹H NMR (500 MHz,
11 DMSO-d₆) : δ 9.75 (br s, 3H), 3.90 (br d, 2H), 3.77 (d, *J* = 10 Hz, 1H), 3.60 (br s, 1H), 3.20 (d, *J*
12 = 10 Hz, 1H), 2.96-3.01 (m, 1H), 2.60-2.73 (m, 1H), 2.28-2.30 (m, 1H), 2.01-2.04 (m, 1H), 1.88-
13 1.94 (m, 1H), 1.72-1.82 (m, 3H), 1.51-1.68 (m, 4H), 1.40 (s, 9H); ¹³C NMR (125 MHz, DMSO-
14 d₆) : δ 171.87, 168.97, 166.83, 153.79, 78.78, 58.57, 57.71, 47.09, 40.40, 28.05, 27.42, 20.33,
15 18.29. Mass: (M-1): 410.3 for C₁₈H₂₉N₅O₆; HPLC purity: 96.34%. Step-3: Tetrabutyl
16 ammonium salt of (2S, 5R)-6-sulfooxy-7-oxo-2-(((3R)-N-Boc-piperidine-3-carbonyl)-
17 hydrazinocarbonyl]-1,6-diaza-bicyclo[3.2.1] oct-ane (**2d**): To the clear mixture of hydroxyl
18 intermediate **2c** (113 gm, 0.274 mol), in dichloromethane (1.13 L) was added triethylamine (77
19 ml, 0.548 mol) followed by sulfurtrioxide pyridine complex (57 gm, 0.356 mol) at 35°C. The
20 reaction mixture was stirred for 3 hr and added 0.5 M aqueous potassium dihydrogen phosphate
21 (1.13 L) followed by ethyl acetate (2.26 L). Aqueous layer was washed with dichloromethane:
22 ethyl acetate mixture (1:2 v/v, 2.26 L twice). The aqueous layer was stirred with solid tetrabutyl
23 ammonium hydrogen sulfate (84 gm, 0.247 mol) for 3 hr. The mixture was extracted with
24 dichloromethane (1.13 L). The organic layer was evaporated under vacuum to provide crude
25 TBA salt. It was purified on a short silica gel column to provide pure intermediate **2d** as a foamy
26
27
28
29
30
31
32
33
34
35
36
37
38
39
40
41
42
43
44
45
46
47
48
49
50
51
52
53
54
55
56
57
58
59
60

1
2
3 white solid in 122 gm (60%) quantity. Analysis of analytical sample: ^1H NMR (400 MHz,
4 CDCl_3) : δ 8.54 (br s, 2H), 4.31 (br s, 1H), 3.98 (d, $J = 8$ Hz, 2H), 3.18-3.37 (m, 12H), 2.45 (br s,
5 1H), 2.32-2.37 (m, 1H), 2.10-2.20 (br m, 1H), 1.83-1.96 (m, 5H), 1.62-1.73 (m, 10H), 1.26-1.49
6 (m, 18H), 1.00 (t, 12H); ^{13}C NMR (100 MHz, CDCl_3) : δ 172.32, 168.50, 165.82, 154.78, 60.22,
7 59.30, 58.40, 57.79, 47.86, 40.68, 28.22, 23.96, 23.70, 20.49, 19.49, 17.28. 13.49; Mass: (M-1):
8 490.4 as a free sulfonic acid for $\text{C}_{18}\text{H}_{28}\text{N}_5\text{O}_9\text{S.N}(\text{C}_4\text{H}_9)_4$; HPLC purity: 96.3%. Step-4 **2**: (2S,
9 5R)-6-sulfooxy-7-oxo-2-[(3R)-piperidine-3-carbonyl]-hydrazinocarbonyl]-1,6-diaza-
10 bicyclo[3.2.1]octane (**2e**): To the clear solution of TBA salt intermediate **2d** (113 gm, 0.154 mol)
11 in dichloromethane (280 ml) was added trifluoroacetic acid (280 ml) between 0°C to 5°C via
12 addition funnel. The excess trifluoroacetic acid and solvent was evaporated under vacuum below
13 40°C to provide pale yellow oily residue. Oily residue was triturated with methyl tert-butyl ether
14 (2.25 L X 2). The precipitate was filtered and was suspended in acetone (1.130 L) and the pH of
15 suspension was adjusted to 5.5 to 6.5 (aliquot slurry was taken out and made a clear solution by
16 adding water prior to measure pH) by adding 10% solution of sodium-2-ethyl hexanoate in
17 acetone. The suspension was filtered and dried under vacuum below 40°C to furnish 65 gm
18 crude **2**. The crude **2** was purified in 15% aqueous isopropanol to provide white crystalline **2** (**2e**)
19 in 48 gm quantity in 80% yield. Analysis of analytical sample: ^1H NMR (400 MHz, DMSO-d_6) :
20 δ 9.99 (br s, 2H), 8.39 (br s, 2H), 4.03 (br s, 1H), 3.84 (d, $J = 6.8$ Hz, 1H), 3.12-3.23 (m, 3H),
21 2.99-3.05 (m, 2H), 2.91 (t, $J = 10$ Hz, 1H), 2.68 (br m, 1H), 1.99-2.05 (m, 1H), 1.57-1.90 (m,
22 7H). ^{13}C NMR (100 MHz, DMSO-d_6): δ 171.1, 168.9, 165.9, 58.3, 57.5, 46.9, 44.3, 43.2, 36.9,
23 25.8, 20.9, 20.5. 18.4. IR (cm^{-1}): 3509, 1749, 1715, 1676, 1279, 1242, 1030. Analysis calculated
24 for **2** dihydrate $\text{C}_{13}\text{H}_{21}\text{N}_5\text{O}_7\text{S}.2\text{H}_2\text{O}$ C, 36.53; H, 5.89; N, 16.39. Found: C, 36.26; H, 5.92; N,
25 16.30. Mass: (M+1): 392.3 for $\text{C}_{13}\text{H}_{21}\text{N}_5\text{O}_7\text{S}$. HPLC purity 98.84%; Column: 5 μm particle size
26
27
28
29
30
31
32
33
34
35
36
37
38
39
40
41
42
43
44
45
46
47
48
49
50
51
52
53
54
55
56
57
58
59
60

1
2
3 Unisol C18 column (Bonna Agela Technologies); mobile phase: buffer (0.01 M ammonium
4 dihydrogen phosphate water and pH adjusted to 7.2 ± 0.1 with dilute ammonia solution) and
5 acetonitrile in gradient mode; detection: at 225 nm. column temperature: 25°C; flow rate: 1
6 mL/min. **2** solution was maintained at 10 °C. Specific rotation: $[\alpha]_D^{25}$: -32.6° (c 0.5, water)
7
8
9

10
11
12
13
14
15
16
17 **Synthesis of (2S, 5R)-1,6-diaza-bicyclo[3.2.1]octane-2-carbonitrile-7-oxo-6-(sulfooxy)- mono**

18 **sodium salt (3)-** Step 1: Preparation of (2S,5R)-6-(benzyloxy)-7-oxo-1,6-diaza-
19 bicyclo[3.2.1]octane-2-carboxamide (**3a**): Triethylamine hydrochloride (104 g, 0.755 mole) was
20 added to a suspension of Sodium (2S, 5R)-6-(benzyloxy)-7-oxo-1,6-diazabicyclo[3.2.1]octane-2-
21 carboxylate A (150 gm, 0.503 mol) in DCM (1.5 L) under stirring at 30°C and after 1 h
22 triethylamine (70 ml, 0.503 mol) was added followed by drop wise addition of pivaloyl chloride
23 (74 ml, 0.603 mol) at 0°C to 5°C and stirring continued further for 1h. The reaction mixture was
24 cooled to -20°C and aqueous ammonia (103 ml, 1.51 mol) was slowly added. After 30 min of
25 stirring at -20°C, water (1.5 L) was added and the two layers separated. The aqueous layer was
26 extracted with fresh DCM (750 ml). The combined organic layer was dried over anhydrous
27 Na₂SO₄ and evaporated under reduced pressure (200 mm Hg). The concentrate was diluted with
28 n-butyl chloride (450 ml) and the mixture stirred for 2 h. The separated solid was filtered and the
29 solid residue washed with fresh n-butyl chloride (100 ml). The solid was dried under reduced
30 pressure (4 mm Hg) to obtain the product (**3a**), as white solid, 55 g, (yield 40 %). Mp: 170-172
31 °C. Analysis of analytical sample: ¹H-NMR (500MHz, CDCl₃): δ 7.42-7.27 (m, 5H), 6.60 (1H,
32 s), 5.71 (s, 1H), 5.06 (d, 1H, J = 10 Hz), 4.91 (d, 1H, J = 10 Hz), 4.95 (d, 1H, J = 10 Hz), 3.32 (s,
33 1H), 3.04 (d, 1H, J = 10 Hz), 2.77 (d, 1H, J = 10 Hz), 2.37-2.33 (1H, m), 2.02-1.92 (m, 2H),
34
35
36
37
38
39
40
41
42
43
44
45
46
47
48
49
50
51
52
53
54
55
56
57
58
59
60

1
2
3 1.62 (1H, m). Mass: (M+1): 276 for C₁₄H₁₇N₃O₃. HPLC purity: 99.11 %. Step 2: Synthesis of
4
5 (2S, 5R)-6-(benzyloxy)-7-oxo-1,6-diaza-bicyclo[3.2.1]octane-2-carbonitrile (**3b**): Trifluoroacetic
6
7 anhydride (48 ml, 0.340 mol) was slowly added to a solution of (2S,5R)-6-(benzyloxy)-7-oxo-
8
9 1,6-diaza-bicyclo[3.2.1]octane-2-carboxamide, **3a** (47.0 g, 0.170 mol), in DCM (1430 ml)
10
11 containing triethylamine (107 ml, 0.765 mol) at -5°C, under stirring. After 2 h of stirring at -5°C,
12
13 water (1450 ml) was added to the reaction mixture and stirring continued for 15 minutes. The
14
15 organic layer was separated and washed with saturated sodium bicarbonate solution (470 ml),
16
17 with brine (470 ml) dried over anhydrous Na₂SO₄ and evaporated under reduced pressure (200
18
19 mm Hg). The crude thus obtained was purified by column chromatography over silica gel (60-
20
21 120 mesh) using 10-20% v/v mixtures of acetone: hexane as an eluent. Evaporation of the
22
23 solvent from the combined fractions, gave the product (**3b**), 32 g as a buff coloured solid (yield
24
25 74%). Mp: 80-82°C. Analysis of analytical sample: ¹H NMR (500MHz, DMSO-d₆): δ 7.41-
26
27 7.38 (m, 5H), 5.06-5.04 (d, 1H, *J* = 8 Hz), 4.91-4.89 (d, 1H, *J* = 8 Hz), 4.38-4.37 (d, 1H, *J* = 4
28
29 Hz), 3.37-3.36 (t, 1H, *J* = 4 Hz), 3.30-3.27 (d, 1H, *J* = 12 Hz), 3.16-3.16 (m, 1H), 2.31-2.27 (m,
30
31 1H), 2.13-2.12 (m, 1H), 1.89-1.81 (m, 2H). Mass: (M+1): 258 for C₁₄H₁₅N₃O₂. HPLC purity:
32
33 100%. Step 3: Synthesis of (2S,5R)-6-hydroxy-7-oxo-1,6-diaza-bicyclo[3.2.1]octane-2-
34
35 carbonitrile (**3c**): A solution of (2S,5R)-6-(benzyloxy)-7-oxo-1,6-diaza-bicyclo[3.2.1]octane-2-
36
37 carbonitrile **3b** (32 g, 0.124 mol) in a mixture of DMF: DCM (1:1, 160 ml:160 ml) containing
38
39 10% Pd/C (4.6 g, 50% wet) was hydrogenated at 50-55 psi, for 2 h, at 25°C. The resulting
40
41 mixture was filtered through a celite pad and residue was washed with DMF: DCM (1:1, 25 ml:
42
43 25 ml). The solvent from the combined filtrate was evaporated under reduced pressure to obtain
44
45 the product as oil, which was used as such for the next reaction without further purification.
46
47 (20.66 g; yield ca ~100%). Small quantity was purified by column chromatography over silica
48
49
50
51
52
53
54
55
56
57
58
59
60

1
2
3 gel (60-120 mesh) and using 30-35% v/v mixture of acetone: hexane as an eluent. Evaporation of
4
5 the solvent from the combined fractions gave the product (**3c**) as a pale yellow solid. Mp: 135-
6
7 140°C. (Dec) Analysis of analytical sample: ¹H NMR (500 MHz, DMSO-d₆): δ 9.97 (s, 1H),
8
9 4.52-4.50 (d, 1H, J =8 Hz), 3.69 (s, 1H), 3.19 (s, 2H), 2.01-2.00 (m, 2H), 1.86-1.83 (m, 2H).
10
11 Mass: (M-1): 166.1 for C₇H₉N₃O₂. HPLC purity: 99.7%. Step 4: Synthesis of (2S, 5R)-6-
12
13 (sulfooxy)-7-oxo-1,6-diaza-bicyclo[3.2.1]octane-2-carbonitrile, tetrabutylammonium salt (**3d**):
14
15 To a stirred and cooled (5 - 10°C) solution of (2S,5R)-6-hydroxy-7-oxo-1,6-diaza-
16
17 bicyclo[3.2.1]octane-2-carbonitrile **3c** (20.66 g, 0.124 mol) in DMF (160ml) DMF-SO₃ complex
18
19 (22.8 g, 0.149 mol) was added in one portion and stirring continued further. After 1h of stirring,
20
21 to the resulting reaction mass was added slowly, a solution of tetrabutylammonium acetate (48.6
22
23 g, 0.161 mol) in water (160 ml). After 1 h of further stirring, the solvent from the reaction
24
25 mixture was evaporated under reduced pressure to obtain an oily residue. The oily mass was co-
26
27 evaporated with xylene (2 x 200 ml), to obtain a thick mass. This mass was partitioned between
28
29 dichloromethane (320 ml) and water (320 ml). The organic layer was separated and the aqueous
30
31 layer re-extracted with dichloromethane (160 ml). The combined organic extracts were washed
32
33 with water (3 x 160 ml), dried over anhydrous Na₂SO₄ and the solvent evaporated under reduced
34
35 pressure at 35 °C. The residual oily mass was triturated with ether (3 x 160 ml), each time the
36
37 ether layer was decanted and finally the residue was dried under reduced pressure, to obtain the
38
39 product (**3d**) as pale yellow oil, 52.5 g (86% yield). Analysis of analytical sample: ¹H NMR
40
41 (400 MHz, CDCl₃): δ 4.42 (s, 1H), 4.34 (d, 1H, J = 6.8 Hz), 3.45 (d, 1H, J = 12.4 Hz), 3.36 (d,
42
43 1H, J =12.4 Hz), 3.31-3.23 (m, 8H),), 2.35-2.20 (2H, m), 1.94-1.81 (2H, m), 1.69-1.56 (8H, m),
44
45 1.48-1.39 (8H, m), 1.02-0.98 (12H, m). Mass: (M-1): 246 as a free sulfonic acid for C₇H₈N₃O₅S.
46
47 N(C₄H₉)₄. HPLC purity: 95.24%. Step 5: Synthesis of (2S, 5R)-1,6-diaza-bicyclo[3.2.1]octane-
48
49
50
51
52
53
54
55
56
57
58
59
60

1
2
3 2-carbonitrile-7-oxo-6-(sulfooxy)- mono sodium salt (**3**): A solution of (2S, 5R)-6-(sulfooxy)-7-
4 oxo-1,6-diaza-bicyclo[3.2.1]octane-2-carbonitrile, tetrabutylammonium salt **3d** (51.5 g, 0.105
5 mol) in THF (50 ml) was loaded on column packed with Indion 225 Na resin (1200 gm) and
6 was eluted by using 10% THF in water. The pure fractions were collected and THF was
7 evaporated under reduced pressure. The aqueous solution was extracted with ethyl acetate (5 x
8 250 ml), treated with charcoal to decolourise and filtered. The filtrate was lyophilised, and the
9 powder obtained was recrystallized using isopropanol: water, to obtain the product (**3**), as a white
10 solid, 20.5 g (72% yield). Mp: 198-201°C. (Dec) Analysis of analytical sample: ¹H NMR
11 (400MHz, DMSO-d₆): δ 4.56-4.54 (d, 1H, J=6.8 Hz), 4.09 (s, 1H), 3.31-3.22 (s, 2H), 1.98-1.86
12 (m, 4H). ¹³C NMR (400MHz, DMSO-d₆): δ 163.5 (C=O), 119.1 (CN), 57.3 (CH), 48.6 (CH),
13 48.0 (CH₂), 22.0 (CH₂), 20.2 (CH₂). IR (cm⁻¹): 3543, 2249, 1751, 1292, 1072, 1020, 1009. Mass:
14 (M-1): 246 as a free sulfonic acid for C₇H₈N₃O₅SNa. HPLC purity: 99.6 %. Water content
15 4.18%. Analysis calculated for **3**, C₇H₈N₃O₅SNa, C, 31.23; H, 3.0; N, 15.61. Found: C, 30.94; H,
16 3.4; N, 15.45. Specific rotation: [α]_D²⁵: -28.7° (c 0.5, water)
17
18
19
20
21
22
23
24
25
26
27
28
29
30
31
32
33
34
35
36
37

38 **Plasmids and Strains.** The cloning and/or origins for *bla*_{KPC-2}, *bla*_{PDC-3}, and *bla*_{ADC-7} genes for
39 susceptibility testing and *bla*_{KPC-2}, *bla*_{PDC-3}, *bla*_{ADC-7}, *bla*_{OXA-23}, and *bla*_{OXA-24/40} genes (missing
40 the nucleotides encoding their signal peptides) for protein expression were described in the
41 following references^{11, 20, 35-37}. The methods for the generation of the *A. baumannii*
42 ATCC17978 knockout strains is previously described³⁸.
43
44
45
46
47
48

49 For MIC analysis, the *bla*_{OXA-48} gene was cloned into the pBC SK (-) vector by
50 amplifying the *bla*_{OXA-48} coding and upstream promoter regions from *K. pneumoniae* CAV1543
51 containing *bla*_{OXA-48}, sequence verified, and transformed into the *E. coli* DH10B¹⁹. For large
52
53
54
55
56
57
58
59
60

1
2
3 scale protein expression, the *bla*_{OXA-48} gene without its leader peptide sequence was cloned into
4
5 the pET24a(+) vector using NdeI and XhoI restriction sites and electroporated into *E. coli*
6
7 DH10B. The resulting construct was sequence verified and transformed into *E. coli* BL21(DE3)
8
9 cells for protein expression and purification.
10
11

12 For MIC testing, as OXA-23 and OXA-24/40 do not express well in an *E. coli*
13
14 background, presumably due to codon usage, another expression strategy was utilized. For
15
16 *bla*_{OXA-23}, the *bla* gene and its upstream ISAbal was amplified from strain AB0057, and for
17
18 *bla*_{OXA-24/40} the *bla* gene and its upstream XerC/XerD was amplified from strain *A. baumannii*
19
20 NM55. The amplified genes were cloned into the XbaI site of the modified pWH1266 vector (a
21
22 vector that replicates in *A. baumannii*) in which ampicillin resistance was eliminated (Δbla_{TEM-1})
23
24 by inverse PCR, and an XbaI site was engineered into the vector. Once the proper sequence was
25
26 confirmed in the constructs, the clone was transformed into *A. baumannii* OM2 clinical isolate.
27
28 To reduce the ampicillin MIC of the OM2 strain, the native *bla*_{ADC} gene was knocked out. A 3
29
30 kb fragment including the *bla*_{ADC} gene and about 1 kb flanking sequence upstream and
31
32 downstream of *bla*_{ADC} was amplified out of OM2 and cloned into pCR-XL-TOPO. The *bla*_{ADC}
33
34 gene in the pCR-XL-TOPO clone was removed by inverse PCR, and a tobramycin resistance
35
36 gene in the pCR-XL-TOPO clone was removed by inverse PCR, and a tobramycin resistance
37
38 gene was put in its place. This plasmid was used to generate the *bla*_{ADC} knockout. Linearized
39
40 *bla*_{ADC} knockout plasmid was electroporated into OM2 cells with selection on tobramycin.
41
42 Colonies that grew on tobramycin were PCR screened for the tobramycin resistance gene to
43
44 assure that they were not breakthrough colonies. PCR using a primer upstream of the area used
45
46 to make the *bla*_{ADC} construct and a second primer residing in the tobramycin resistance gene was
47
48 performed to show integration into the desired location. Finally, PCR to amplify the *bla*_{ADC} gene
49
50 was negative, demonstrating that the *bla*_{ADC} gene was successfully knocked out. Note: The
51
52
53
54
55
56
57
58
59
60

1
2
3 *bla*_{ADC} knockout of OM2 still contains *bla*_{OXA-51}. Numerous attempts to knock out the *bla*_{OXA-51}
4 gene were unsuccessful. It is unknown if other β -lactamases are present in OM2.
5
6
7
8
9

10 **Protein Purification for Kinetic Assays and Mass Spectrometry.** The purification of KPC-2,
11 ADC-7, PDC-3, and OXA-23 was previously described^{11, 20, 36, 37}. OXA-24/40, and OXA-48
12 were purified according to the following protocols.
13
14
15

16
17 The OXA-24/40 β -lactamase was purified as follows. *E. coli* BL21(DE3) containing
18 *bla*_{OXA-24/40} pET24 (+) construct was grown in SOB containing 50 μ g/ml kanamycin at 37 °C
19 shaking to achieve an OD₆₀₀ of 0.8. IPTG was added to the culture to a final concentration of 0.2
20 mM and the culture was grown for three more hours. The cells were centrifuged and frozen at -
21 20 °C. Pellets were thawed and suspended in 50 mM Tris-HCl, pH 7.4 with lysozyme (40
22 μ g/ml), benzonuclease, and 1 mM MgSO₄. Cellular debris was removed by centrifugation, and
23 the lysate was subjected to preparative isoelectric focusing (pIEF) overnight. Location of OXA-
24 24/40 on the pIEF gel was determined using a nitrocefin (NCF; Becton, Dickinson and
25 Company) overlay. OXA-24/40 further purified by SEC using a HiLoad 16/60 Superdex 75
26 column (GE Healthcare Life Science). The OXA-48 β -lactamase was purified from *E. coli*
27 BL21(DE3) containing *bla*_{OXA-48}/ pET24 (+) construct as described above for OXA-24/40.
28
29
30
31
32
33
34
35
36
37
38
39
40
41
42
43
44

45 **Steady-State Inhibitor Kinetics.** To determine the inhibitory potential of compounds **1**, **2**, and **3**
46 against select class A, C, and D β -lactamases, steady-state inhibition kinetics were conducted
47 using an Agilent 8453 Diode Array spectrophotometer. Class A and C β -lactamases were tested
48 in 10 mM phosphate-buffered saline, pH 7.4, while 50 mM sodium phosphate buffer, pH 7.2
49
50
51
52
53
54
55
56
57
58
59
60

(supplemented with 20 mM sodium bicarbonate) was used for class D β -lactamases³⁹. The proposed interactions between β -lactamases and DBOs is depicted in **Figure 3A**.

As an initial screen for inhibitor, a direct competition assay was performed to estimate the Michaelis constant, $K_{i \text{ app}}$ of the inhibitor. If the $K_{i \text{ app}}$ value was $>100 \mu\text{M}$, further biochemical analyses were not pursued. We used a final concentration of 50-100 μM (or 3-5 $\times K_m$) of nitrocefin (ncf) as the indicator substrate and nM concentrations of β -lactamase in these determinations. The data were analyzed according to equation 1 to account for the affinity of nitrocefin for the β -lactamase: $K_{i \text{ app}} (\text{corrected}) = K_{i \text{ app}} (\text{observed}) / (1 + [\text{S}] / K_m \text{ nitrocefin})$ (Eq. 1). Where, [S] is the concentration of nitrocefin.

The second-order rate constant for enzyme and inhibitor complex inactivation, k_2/K , was measured directly by monitoring the reaction time courses in the presence of inhibitor. A fixed concentration of enzyme, nitrocefin, and increasing nM concentrations of BLI or BLE were used in each assay. Progress curves were fit to equation 2 to obtain the observed rate constant for inactivation (k_{obs}): $y = V_f \cdot x + (V_0 - V_f) \cdot [1 - \exp(-k_{\text{obs}} \cdot X)] / k_{\text{obs}} + A_0$ (Eq. 2)

Here, V_f is the final velocity, V_0 is the initial velocity, and A_0 is the initial absorbance at wavelength = 482 nm. Data were plotted as k_{obs} vs. [I]. The k_2/K values were obtained by correcting the value obtained for the slope of the line (k_2/K observed) for the use of the K_m of ncf for the given enzyme according to equation 3: $k_2 / K (\text{corrected}) = k_2 / K (\text{observed}) \cdot ([\text{S}] / K_m \text{ ncf}) + 1$ (Eq. 3)

The off rate or k_{off} was determined by incubating β -lactamase with DBOs at a concentration of $5 \times K_{i \text{ app}}$ for 30 min. Samples were serially diluted and hydrolysis of 100 μM nitrocefin was measured. The progress curves were fit to a single exponential decay equation.

1
2
3 Partition ratios ($k_{\text{cat}}/k_{\text{inact}}$ [where k_{inact} is the rate constant of enzyme inactivation]) at 24 hr
4
5 for β -lactamases with inhibitor were obtained by incubating enzyme with increasing
6
7 concentrations of inhibitor at room temperature. The ratio of inhibitor to enzyme ($I:E$) necessary
8
9 to inhibit the hydrolysis of NCF by >99% were determined.
10
11
12
13

14 **Mass Spectrometry.** Electrospray ionization mass spectrometry (ESI-MS) of the intact β -
15
16 lactamases was performed on a Waters SynaptG2-Si quadrupole-time-of-flight mass
17
18 spectrometer. The Synapt G2-Si was calibrated with sodium iodide using a 50-2000 m/z mass
19
20 range. This calibration resulted in an error of ± 5 amu. After 5 min and 24 hr incubation of β -
21
22 lactamase and inhibitor at 1:1 ratio, the reactions were terminated by the addition of 0.1% formic
23
24 acid and 1% acetonitrile. The samples were run using a Waters Acquity H class Ultra
25
26 Performance Liquid Chromatography (UPLC) on an Acquity UPLC BEH C18 1.7 μm , 2.1x100
27
28 mm column. The mobile phase consisted of 0.1% formic acid in water. The tune settings for
29
30 each data run are as follows: capillary voltage at 3.2kV, sampling cone at 30V, source offset at
31
32 30, source temperature at 100°C, desolvation temperature at 450°C, cone gas at 50 L/hr,
33
34 desolvation gas at 600 L/hr, and nebulizer bar at 6.0. Spectra will be analyzed using MassLynx
35
36 v4.1. Data presented are the consensus results from 2-3 experiments.
37
38
39
40
41

42 To determine if any resulting adducts (e.g., -80 amu, see Results) were mass
43
44 spectrometry artifacts, samples were re-run using capillary voltages of 1kV or 4.5kV with the
45
46 other conditions as described above. In addition, the samples were re-run with the sampling
47
48 cone at 5V, 20V, 30V, 40V, 50V, 60V, or 70V with the other conditions as described above⁴.
49
50
51
52
53
54
55
56
57
58
59
60

1
2
3 **Acyl Transfer.** To assess if the **1**, **2**, and **3** recyclize to reform active compound, an acyl-transfer
4
5 ESI-MS experiment was conducted using KPC-2 as the donor and TEM-1 as the recipient. 5 μM
6
7 KPC-2 was incubated with **1**, **2**, or **3** at a equimolar ratio for 1 min. 5 μM TEM-1 β -lactamase
8
9 was added to the mixture. At the time points of 15 sec and 5 min, reactions were terminated and
10
11 prepared for ESI-MS as described above.
12
13
14
15
16

17 **Protein Purification for Crystallography.** KPC-2 was expressed and purified as described
18
19 previously^{40, 41}. The purified KPC-2 protein was concentrated to 10 mg/mL (measured by
20
21 Bradford assay), aliquoted, and stored at -80°C until further use for co-crystallization or soaking
22
23 of the **1**, **2**, or **3** inhibitors as described below. OXA-24/40 was expressed and purified as
24
25 previously described²³.
26
27
28
29
30

31 **Crystallization of Apo KPC-2 and Soaking of 1, 2, and 3.** KPC-2 crystals were grown in the
32
33 same crystallization condition as described previously²², which consists of 20% PEG6000, 100
34
35 mM citrate pH 4.0, and 100 mM KSCN, yet 10 mM CdCl_2 was added as a crystallization
36
37 additive to improve crystallization. The addition of CdCl_2 also favored KPC-2 to crystallized in
38
39 the P1 spacegroup. Protein concentration for crystallization was 10 mg/ml. The soaking
40
41 solutions were prepared similarly to crystallization conditions at pH 5.0 with an addition of 10
42
43 mM inhibitor (**1**, **2**, and **3**). The KPC-2 crystals were soaked for 3 hours before being cryo-
44
45 protected with the soaking solution containing also 20% ethylene glycol and subsequently flash
46
47 frozen in liquid nitrogen prior to data collection.
48
49
50
51
52
53
54
55
56
57
58
59
60

1
2
3 **Co-Crystallization of KPC-2 with 1, 2, and 3.** Prior to co-crystallization, the KPC-2 protein
4 and each inhibitor were incubated for 40 min with a protein to inhibitor molar ratio of 1 is to 10
5 (KPC-2 concentration was 10 mg/mL). The KPC-2:inhibitor co-crystals were crystallized using
6 200 mM lithium sulfate, 100 mM sodium acetate pH 4.4-4.6, and 28-31% PEG8000. After
7 growing to final in about 3 days, the co-crystals were mounted and cryo-protected with
8 perfluoropolyether (Hampton Research) prior to flash freezing in liquid nitrogen.
9
10
11
12
13
14
15
16
17
18

19 **Co-Crystallization of OXA-24/40 with 3.** OXA-24/40 was pre-incubated with 3 overnight with
20 a 1:50 molar ratio of protein to inhibitor. The OXA-24/40:3 complex was crystallized in 0.2 M
21 calcium acetate, 0.2 M sodium cacodylate pH 6.5, and 18% PEG8000. Crystals were cryo-
22 protected using the mother liquor before freezing in liquid nitrogen prior to data collection.
23
24
25
26
27
28
29
30

31 **X-ray Data Collection and Crystallographic Refinement.** Data for the KPC-2: 1, 2, and 3
32 complexes were collected at the SSRL beamline. The data for the OXA-24/40:3 complex was
33 collected at APS. All datasets were processed using AutoXDS scripts^{42, 43} and the protein
34 structures were refined using Refmac⁴⁴ and Coot programs⁴⁵. The starting protein coordinates
35 for all KPC-2 structures in this study was KPC-2 in complex with 3-NPBA (PDB ID 3RXX) and
36 for the OXA-24/40 starting structure was 4WM9. The KPC-2 structures have two molecules in
37 the asymmetric structure whereas there is only 1 molecule in the asymmetric unit in the OXA-
38 24/40 structure. The structures in the two different molecules in each KPC-2 complex structure
39 are very similar so for the most part, only molecule A will be discussed. The chemical structures
40 of inhibitors, their corresponding parameter and topology files were generated using PRODRG
41 program⁴⁶. The coordinates were checked using the structure validation program PROCHECK⁴⁷
42
43
44
45
46
47
48
49
50
51
52
53
54
55
56
57
58
59
60

1
2
3 and found to have no outliers in the Ramachandran plot. The coordinates and structure factors of
4
5 the structures have been deposited with the Protein Data Bank and the PDB identifiers are listed
6
7 in **Table S1**.
8
9

10
11
12 **Susceptibility Testing.** MICs for various bacterial isolates were determined by broth
13
14 microdilution method using custom frozen panels (ThermoFisher Scientific, Cleveland, OH)
15
16 according to the Clinical and Laboratory Standards Institute guidelines^{48, 49}. **1, 2, 3**, avibactam,
17
18 relebactam, meropenem and cefepime were tested alone. **1, 2**, and **3** were tested at 4 mg/L and 8
19
20 mg/L while avibactam and relebactam were tested at 4 mg/L in combination with increasing
21
22 concentrations of meropenem and cefepime. MICs were performed in triplicate and modal
23
24 values reported.
25
26
27
28
29

30
31 **Murine Peritonitis Model.** Male and female Swiss albino mice were intraperitoneally infected
32
33 with a bacterial inoculum (3.5×10^5 to 3×10^6 CFU/mouse) resuspended in 5% hog gastric mucin
34
35 that resulted in mortality of untreated animals within 24 hr. Subcutaneous treatment of drugs was
36
37 initiated 1h post-infection for 1 day. Cefepime, cefepime-**2**, meropenem-cilastatin, meropenem-
38
39 cilastatin-**3** and tigecycline werer given as two doses (3 hr apart) and colistin was given three
40
41 doses (3 hr apart). Survival patterns were monitored for 7 days. The $PD_{50/90}$ values were
42
43 determined by probit analysis. All animal experiments performed in the manuscript were
44
45 conducted in compliance with Wockhardt Research Centre guidelines.
46
47
48
49

50
51 **Neutropenic Murine Lung Infection Model.** Male and female Swiss mice weighing 25-27 g
52
53 were rendered neutropenic by intraperitoneal administration of cyclophosphamide (150 and 100
54
55
56
57
58
59
60

1
2
3 mg/kg; 1 and 4 days prior to infection). Two hours prior to the initiation of antimicrobial therapy,
4
5 intranasal infection was caused by instilling 80 μL of bacterial suspension (10^5 - 10^6 \log_{10}
6
7 CFU/mL) of Indian clinical isolate *A. baumannii* SL04 expressing *bla*_{OXA-23}. A group of 6 mice
8
9 were administered humanized doses of cefepime, **2**, and meropenem:cilastatin by subcutaneous
10
11 route in fractionated regimen. **3** was also administered as fractionated doses in combination with
12
13 meropenem:cilastatin. Imipenem:cilastatin and relebactam were administered at their simulated
14
15 clinical doses. Doses were fractionated as q2h regimen. Lungs from all the animals including
16
17 untreated animals, were harvested 3 hr post last dose of q2h regimen and individually
18
19 homogenized (Homogenizer, IKA – Ultra Turrax T 25) in 3 mL normal saline. One hundred
20
21 microliters of this homogenate was diluted serially and plated on trypticase soy agar plates and
22
23 the colonies appearing following incubation at 37°C for 18 h were counted. Bacterial load of
24
25 untreated animals enumerated at the time of initiation of therapy (2 hr post infections) served as
26
27 reference count to quantify the magnitude of antibacterial effect realized through various dosing
28
29 regimens. Bacterial load at initiation of treatment (2 hr post infection) was $6.13 \pm 0.17 \log_{10}$
30
31 CFU/lung, which increased to $7.62 \pm 1.22 \log_{10}$ CFU/lung at 27 h post infection. All animal
32
33 experiments performed in the manuscript were conducted in compliance with Wockhardt
34
35 Research Centre guidelines.
36
37
38
39
40
41
42
43

44 ASSOCIATED CONTENT

45 46 47 48 Accession Codes

49 Authors will release the atomic coordinates and experimental data upon article publication.
50
51
52
53
54
55
56
57
58
59
60

1
2
3 KPC-2 soaked **1** (PDB#: 6B1X); KPC-2 soaked **2** (PDB#: 6B1J); KPC-2 soaked **3** (PDB#:
4 6B1F); KPC-2 co-crystallized **1** (PDB#: 6B1Y); KPC-2 co-crystallized **2** (PDB#: 6B1W); KPC-
5
6
7
8 2 co-crystallized **3** (PDB#: 6B1H); OXA-24/40 co-crystallized **3** (PDB#: 6B22).
9
10
11

12 **AUTHOR INFORMATION**

13 **Corresponding Authors**

14
15
16
17 Phone: 216-791-3800x6230. Email: Krisztina.Papp@va.gov

18
19 Phone: 216-368-8511. Email: fxv5@case.edu

20
21
22 Phone: 216-791-3800x4801. E-mail: Robert.Bonomo@va.gov

23 **ORCID**

24
25
26
27
28
29
30
31
32
33
34
35
36
37
38
39
40
41
42
43
44
45
46
47
48
49
50
51
52
53
54
55
56
57
58
59
60
Krisztina M. Papp-Wallace: 0000-0002-9976-7898

Focco van den Akker: 0000-0001-9210-3565

Robert A. Bonomo: 0000-0002-3299-894X

61 **Author Contributions**

62
63
64
65
66
67
68
69
70
71
72
73
74
75
76
77
78
79
80
81
82
83
84
85
86
87
88
89
90
91
92
93
94
95
96
97
98
99
100
101
102
103
104
105
106
107
108
109
110
111
112
113
114
115
116
117
118
119
120
121
122
123
124
125
126
127
128
129
130
131
132
133
134
135
136
137
138
139
140
141
142
143
144
145
146
147
148
149
150
151
152
153
154
155
156
157
158
159
160
161
162
163
164
165
166
167
168
169
170
171
172
173
174
175
176
177
178
179
180
181
182
183
184
185
186
187
188
189
190
191
192
193
194
195
196
197
198
199
200
201
202
203
204
205
206
207
208
209
210
211
212
213
214
215
216
217
218
219
220
221
222
223
224
225
226
227
228
229
230
231
232
233
234
235
236
237
238
239
240
241
242
243
244
245
246
247
248
249
250
251
252
253
254
255
256
257
258
259
260
261
262
263
264
265
266
267
268
269
270
271
272
273
274
275
276
277
278
279
280
281
282
283
284
285
286
287
288
289
290
291
292
293
294
295
296
297
298
299
300
301
302
303
304
305
306
307
308
309
310
311
312
313
314
315
316
317
318
319
320
321
322
323
324
325
326
327
328
329
330
331
332
333
334
335
336
337
338
339
340
341
342
343
344
345
346
347
348
349
350
351
352
353
354
355
356
357
358
359
360
361
362
363
364
365
366
367
368
369
370
371
372
373
374
375
376
377
378
379
380
381
382
383
384
385
386
387
388
389
390
391
392
393
394
395
396
397
398
399
400
401
402
403
404
405
406
407
408
409
410
411
412
413
414
415
416
417
418
419
420
421
422
423
424
425
426
427
428
429
430
431
432
433
434
435
436
437
438
439
440
441
442
443
444
445
446
447
448
449
450
451
452
453
454
455
456
457
458
459
460
461
462
463
464
465
466
467
468
469
470
471
472
473
474
475
476
477
478
479
480
481
482
483
484
485
486
487
488
489
490
491
492
493
494
495
496
497
498
499
500
501
502
503
504
505
506
507
508
509
510
511
512
513
514
515
516
517
518
519
520
521
522
523
524
525
526
527
528
529
530
531
532
533
534
535
536
537
538
539
540
541
542
543
544
545
546
547
548
549
550
551
552
553
554
555
556
557
558
559
560
561
562
563
564
565
566
567
568
569
570
571
572
573
574
575
576
577
578
579
580
581
582
583
584
585
586
587
588
589
590
591
592
593
594
595
596
597
598
599
600
601
602
603
604
605
606
607
608
609
610
611
612
613
614
615
616
617
618
619
620
621
622
623
624
625
626
627
628
629
630
631
632
633
634
635
636
637
638
639
640
641
642
643
644
645
646
647
648
649
650
651
652
653
654
655
656
657
658
659
660
661
662
663
664
665
666
667
668
669
670
671
672
673
674
675
676
677
678
679
680
681
682
683
684
685
686
687
688
689
690
691
692
693
694
695
696
697
698
699
700
701
702
703
704
705
706
707
708
709
710
711
712
713
714
715
716
717
718
719
720
721
722
723
724
725
726
727
728
729
730
731
732
733
734
735
736
737
738
739
740
741
742
743
744
745
746
747
748
749
750
751
752
753
754
755
756
757
758
759
760
761
762
763
764
765
766
767
768
769
770
771
772
773
774
775
776
777
778
779
780
781
782
783
784
785
786
787
788
789
790
791
792
793
794
795
796
797
798
799
800
801
802
803
804
805
806
807
808
809
810
811
812
813
814
815
816
817
818
819
820
821
822
823
824
825
826
827
828
829
830
831
832
833
834
835
836
837
838
839
840
841
842
843
844
845
846
847
848
849
850
851
852
853
854
855
856
857
858
859
860
861
862
863
864
865
866
867
868
869
870
871
872
873
874
875
876
877
878
879
880
881
882
883
884
885
886
887
888
889
890
891
892
893
894
895
896
897
898
899
900
901
902
903
904
905
906
907
908
909
910
911
912
913
914
915
916
917
918
919
920
921
922
923
924
925
926
927
928
929
930
931
932
933
934
935
936
937
938
939
940
941
942
943
944
945
946
947
948
949
950
951
952
953
954
955
956
957
958
959
960
961
962
963
964
965
966
967
968
969
970
971
972
973
974
975
976
977
978
979
980
981
982
983
984
985
986
987
988
989
990
991
992
993
994
995
996
997
998
999
1000

51 **Notes**

1
2
3 Satish Bhavsar, Tadiparthi Ravikumar, Prasad K. Deshpande, Vijay Patil, Ravindra Yeole,
4
5 Sachin S. Bhagwat, and Mahesh V. Patel are employees of Wockhardt Research Centre,
6
7 Aurangabad, India. The remaining authors do not have any competing financial interests to
8
9 declare.
10
11
12
13

14 **Supporting Information**

15
16
17 Tables S1-S2, Figure S1, and SMILES.
18
19
20

21 **ACKNOWLEDGEMENTS**

22
23 This study was funded by an industry grant from Wockhardt Research Centre (WRC) to KMPW,
24
25 MRJ, FvdA, and RAB. WRC also supplied compounds **1**, **2**, **3**, avibactam, and relebactam
26
27 powders for this work. Research reported in this publication was supported in part by funds
28
29 and/or facilities provided by the Cleveland Department of Veterans Affairs, the Veterans Affairs
30
31 Merit Review Program BX002872 (KMP-W) and BX001974 (RAB) from the United States
32
33 (U.S.) Department of Veterans Affairs Biomedical Laboratory Research and Development
34
35 Service, and the Geriatric Research Education and Clinical Center VISN 10 to RAB. PNR is also
36
37 supported by grants from the Merit Review program and a Research Career Scientist Award,
38
39 both from Department of Veterans Affairs. The contents do not represent the views of the U.S.
40
41 Department of Veterans Affairs or the United States Government. The National Institute of
42
43 Allergy and Infectious Diseases (NIAID) of the National Institutes of Health (NIH) under Award
44
45 Numbers R21AI114508, R01AI100560, R01AI063517, and R01AI072219 to RAB and NIAID
46
47 of NIH Centers of Excellence for Translational Research (CETR) U19 AI109713 Supplemental
48
49 Research Project to KMPW. The content is solely the responsibility of the authors and does not
50
51 necessarily represent the official views of the National Institutes of Health. We would like to
52
53
54
55
56
57
58
59
60

1
2
3 thank the beamline personnel at SSRL for help with data collection. In addition, we thank David
4
5 Lodowski and APS for help with collecting the OXA-24 data set.
6
7
8
9

10 **ABBREVIATIONS USED**

11
12 MDR, multi-drug resistant; DBO, diazabicyclooctane; CRE, carbapenem-resistant
13
14 Enterobacteriaceae; KPC, *Klebsiella pneumoniae* carbapenemase; PDC, *Pseudomonas*-derived
15
16 cephalosporinase; ADC, *Acinetobacter*-derived cephalosporinase; BLI, β -lactamase inhibitors;
17
18 BLE, β -lactam enhancer; PBP, penicillin binding protein; IRT, inhibitor-resistant TEM; IRS,
19
20 inhibitor-resistant SHV; SAR, structure activity relationships; BCH, bicyclo hydrazide; MIC,
21
22 minimum inhibitory concentration; ColS, colistin susceptible; ColR, colistin resistant; RND,
23
24 Resistance-Nodulation-Division; MFP, membrane fusion protein; OMP, outer membrane
25
26 protein; CFU, colony forming units; preparative isoelectric focusing, pIEF; nitrocefin, NCF;
27
28
29
30
31
32

33 **REFERENCES**

- 34
35
36 1. Tacconelli, E.; Carrara, E.; Savoldi, A.; Harbarth, S.; Mendelson, M.; Monnet, D. L.;
37
38 Pulcini, C.; Kahlmeter, G.; Kluytmans, J.; Carmeli, Y.; Ouellette, M.; Outtersson, K.; Patel, J.;
39
40 Cavaleri, M.; Cox, E. M.; Houchens, C. R.; Grayson, M. L.; Hansen, P.; Singh, N.;
41
42 Theuretzbacher, U.; Magrini, N.; Group, W. H. O. P. P. L. W. Discovery, research, and
43
44 development of new antibiotics: the WHO priority list of antibiotic-resistant bacteria and
45
46 tuberculosis. *Lancet Infect Dis* **2018**, *18*, 318-327.
47
48
49 2. Papp-Wallace, K. M.; Bonomo, R. A. New β -lactamase inhibitors in the clinic. *Infectious*
50
51 *disease clinics of North America* **2016**, *30*, 441-464.
52
53
54
55
56
57
58
59
60

- 1
2
3 3. Bonomo, R. A.; Liu, J.; Chen, Y.; Ng, L.; Hujer, A. M.; Anderson, V. E. Inactivation of
4
5 CMY-2 β -lactamase by tazobactam: initial mass spectroscopic characterization. *Biochim Biophys*
6
7 *Acta* **2001**, *1547*, 196-205.
8
9
- 10 4. Ehmann, D. E.; Jahic, H.; Ross, P. L.; Gu, R. F.; Hu, J.; Durand-Réville, T. F.; Lahiri, S.;
11
12 Thresher, J.; Livchak, S.; Gao, N.; Palmer, T.; Walkup, G. K.; Fisher, S. L. Kinetics of
13
14 avibactam inhibition against class A, C, and D β -lactamases. *J Biol Chem* **2013**, *288*, 27960-
15
16 27971.
17
18
- 19 5. Ehmann, D. E.; Jahic, H.; Ross, P. L.; Gu, R. F.; Hu, J.; Kern, G.; Walkup, G. K.; Fisher,
20
21 S. L. Avibactam is a covalent, reversible, non- β -lactam β -lactamase inhibitor. *Proc Natl Acad*
22
23 *Sci U S A* **2012**, *109*, 11663-11668.
24
25
- 26 6. King, D. T.; King, A. M.; Lal, S. M.; Wright, G. D.; Strynadka, N. C. Molecular
27
28 mechanism of avibactam-mediated β -lactamase inhibition. *ACS Infect Dis* **2015**, *1* 175-184.
29
30
- 31 7. Lahiri, S. D.; Walkup, G. K.; Whiteaker, J. D.; Palmer, T.; McCormack, K.; Tanudra, M.
32
33 A.; Nash, T. J.; Thresher, J.; Johnstone, M. R.; Hajec, L.; Livchak, S.; McLaughlin, R. E.; Alm,
34
35 R. A. Selection and molecular characterization of ceftazidime/avibactam-resistant mutants in
36
37 *Pseudomonas aeruginosa* strains containing derepressed AmpC. *J Antimicrob Chemother* **2015**,
38
39 *70*, 1650-1658.
40
41
- 42 8. King, A. M.; King, D. T.; French, S.; Brouillette, E.; Asli, A.; Alexander, J. A.;
43
44 Vuckovic, M.; Maiti, S. N.; Parr, T. R., Jr.; Brown, E. D.; Malouin, F.; Strynadka, N. C.; Wright,
45
46 G. D. Structural and kinetic characterization of diazabicyclooctanes as dual inhibitors of both
47
48 serine- β -lactamases and penicillin-binding proteins. *ACS Chem Biol* **2016**, *11*, 864-868.
49
50
51
52
53
54
55
56
57
58
59
60

- 1
2
3 9. Mushtaq, S.; Warner, M.; Livermore, D. M. In vitro activity of ceftazidime+NXL104
4 against *Pseudomonas aeruginosa* and other non-fermenters. *J Antimicrob Chemother* **2010**, *65*,
5 2376-2381.
6
7
8
9
10 10. Blizzard, T. A.; Chen, H.; Kim, S.; Wu, J.; Bodner, R.; Gude, C.; Imbriglio, J.; Young,
11 K.; Park, Y. W.; Ogawa, A.; Raghoobar, S.; Hairston, N.; Painter, R. E.; Wisniewski, D.; Scapin,
12 G.; Fitzgerald, P.; Sharma, N.; Lu, J.; Ha, S.; Hermes, J.; Hammond, M. L. Discovery of MK-
13 7655, a β -lactamase inhibitor for combination with Primaxin(R). *Bioorg Med Chem Lett* **2014**,
14 24, 780-785.
15
16
17
18
19
20
21 11. Moya, B.; Barcelo, I. M.; Bhagwat, S.; Patel, M.; Bou, G.; Papp-Wallace, K. M.;
22 Bonomo, R. A.; Oliver, A. WCK 5107 (Zidebactam) and WCK 5153 are novel inhibitors of
23 PBP2 showing potent " β -lactam enhancer" activity against *Pseudomonas aeruginosa*, including
24 multidrug-resistant metallo- β -lactamase-producing high-risk clones. *Antimicrob Agents*
25 *Chemother* **2017**, *61*, e02529-16, 1-12.
26
27
28
29
30
31
32
33 12. Morinaka, A.; Tsutsumi, Y.; Yamada, M.; Suzuki, K.; Watanabe, T.; Abe, T.; Furuuchi,
34 T.; Inamura, S.; Sakamaki, Y.; Mitsuhashi, N.; Ida, T.; Livermore, D. M. OP0595, a new
35 diazabicyclooctane: mode of action as a serine β -lactamase inhibitor, antibiotic and β -lactam
36 'enhancer'. *J Antimicrob Chemother* **2015**, *70*, 2779-2786.
37
38
39
40
41
42
43 13. Durand-Reville, T. F.; Guler, S.; Comita-Prevoir, J.; Chen, B.; Bifulco, N.; Huynh, H.;
44 Lahiri, S.; Shapiro, A. B.; McLeod, S. M.; Carter, N. M.; Moussa, S. H.; Velez-Vega, C.;
45 Olivier, N. B.; McLaughlin, R.; Gao, N.; Thresher, J.; Palmer, T.; Andrews, B.; Giacobbe, R. A.;
46 Newman, J. V.; Ehmman, D. E.; de Jonge, B.; O'Donnell, J.; Mueller, J. P.; Tommasi, R. A.;
47 Miller, A. A. ETX2514 is a broad-spectrum β -lactamase inhibitor for the treatment of drug-
48
49
50
51
52
53
54
55
56
57
58
59
60

1
2
3 resistant Gram-negative bacteria including *Acinetobacter baumannii*. *Nat Microbiol* **2017**, *2*,
4
5 17104, 1-10.
6

7
8 14. Mushtaq, S.; Vickers, A.; Woodford, N.; Livermore, D. M. WCK 4234, a novel
9
10 diazabicyclooctane potentiating carbapenems against Enterobacteriaceae, *Pseudomonas* and
11
12 *Acinetobacter* with class A, C and D β -lactamases. *J Antimicrob Chemother* **2017**, *72*, 1688-
13
14 1695.
15

16
17 15. Deshpande, P. K.; Bhavsar, S. B.; Joshi, S. N.; Pawar, S. S.; Kale, R. P.; Mishra, A. M.;
18
19 Jadhav, S. B.; Pavase, L. P.; Gupta, S. V.; Yeole, R. D.; Rane, V. P.; Ahirrao, V. K.; Bhagwat, S.
20
21 S.; Patel, M. V. F-479: WCK 5107 (Zidebactam, ZID): Structure activity relationship (SAR) of
22
23 novel bicyclo acyl hydrazide (BCH) pharmacophore active against Gram negative including
24
25 *Pseudomonas aeruginosa*. In *ASM Microbe* Boston, MA, 2016.
26
27

28
29 16. Pawar, S. S.; Jadhav, S. B.; Mishra, A. M.; Rane, V. P.; Bhawsar, S.; Deshpande, P. K.;
30
31 Yeole, R. D.; Patel, M. V. A Process for Preparation of (2S, 5R)-7-Oxo-6-Sulphooxy-2-(((3R)-
32
33 pPyrrolidine-3-Carbonyl)-Hydrazino Carbonyl]-1,6-Diaza-Bicyclo[3.2.1]octane.
34
35 US20160002234A1 2014.
36
37

38
39 17. Joshi, S.; Jadhav, S. B.; Rane, V. P.; Bhawsar, S.; Deshpande, P. K.; Yeole, R. D.; Patel,
40
41 M. V. A Process for Preparation of (2S, 5R)-6-Sulphooxy-7-Oxo-2-(((3R)-Piperidine-3-
42
43 Carbonyl)-Hydrazino Carbonyl]-1,6-Diaza-Bicyclo[3.2.1] octane. WO 2015110885A1, 2014.
44

45
46 18. Fleming, F. F.; Yao, L.; Ravikumar, P. C.; Funk, L.; Shook, B. C. Nitrile-containing
47
48 pharmaceuticals: efficacious roles of the nitrile pharmacophore. *J Med Chem* **2010**, *53*, 7902-
49
50 7917.
51
52
53
54
55
56
57
58
59
60

- 1
2
3 19. Mathers, A. J.; Hazen, K. C.; Carroll, J.; Yeh, A. J.; Cox, H. L.; Bonomo, R. A.; Sifri, C.
4
5 D. First clinical cases of OXA-48-producing carbapenem-resistant *Klebsiella pneumoniae* in the
6
7 United States: the "menace" arrives in the new world. *J Clin Microbiol* **2013**, *51*, 680-683.
8
9
10 20. Papp-Wallace, K. M.; Bethel, C. R.; Distler, A. M.; Kasuboski, C.; Taracila, M.;
11
12 Bonomo, R. A. Inhibitor resistance in the KPC-2 β -lactamase, a preeminent property of this class
13
14 A β -lactamase. *Antimicrob Agents Chemother* **2010**, *54*, 890-897.
15
16
17 21. Ehmann, D. E.; Jahic, H.; Ross, P. L.; Gu, R. F.; Hu, J.; Durand-Reville, T. F.; Lahiri, S.;
18
19 Thresher, J.; Livchak, S.; Gao, N.; Palmer, T.; Walkup, G. K.; Fisher, S. L. Kinetics of
20
21 avibactam inhibition against class A, C, and D β -lactamases. *J Biol Chem* **2013**, *288*, 27960-
22
23 27971.
24
25
26 22. Krishnan, N. P.; Nguyen, N. Q.; Papp-Wallace, K. M.; Bonomo, R. A.; van den Akker, F.
27
28 Inhibition of *Klebsiella* β -lactamases (SHV-1 and KPC-2) by avibactam: a structural study. *PLoS*
29
30 *One* **2015**, *10*, e0136813.
31
32
33 23. Bou, G.; Santillana, E.; Sheri, A.; Beceiro, A.; Sampson, J. M.; Kalp, M.; Bethel, C. R.;
34
35 Distler, A. M.; Drawz, S. M.; Pagadala, S. R.; van den Akker, F.; Bonomo, R. A.; Romero, A.;
36
37 Buynak, J. D. Design, synthesis, and crystal structures of 6-alkylidene-2'-substituted penicillanic
38
39 acid sulfones as potent inhibitors of *Acinetobacter baumannii* OXA-24 carbapenemase. *J Am*
40
41 *Chem Soc* **2010**, *132*, 13320-13331.
42
43
44 24. Werner, J. P.; Mitchell, J. M.; Taracila, M. A.; Bonomo, R. A.; Powers, R. A. Exploring
45
46 the potential of boronic acids as inhibitors of OXA-24/40 β -lactamase. *Protein Sci* **2017**, *26*,
47
48 515-526.
49
50
51 25. Lahiri, S. D.; Mangani, S.; Jahic, H.; Benvenuti, M.; Durand-Reville, T. F.; De Luca, F.;
52
53 Ehmann, D. E.; Rossolini, G. M.; Alm, R. A.; Docquier, J. D. Molecular basis of selective
54
55
56
57
58
59
60

1
2
3 inhibition and slow reversibility of avibactam against class D carbapenemases: a structure-
4 guided study of OXA-24 and OXA-48. *ACS Chem Biol* **2014**, 10.1021/cb500703p.
5

6
7
8 26. Vercheval, L.; Bauvois, C.; di Paolo, A.; Borel, F.; Ferrer, J. L.; Sauvage, E.; Matagne,
9 A.; Frere, J. M.; Charlier, P.; Galleni, M.; Kerff, F. Three factors that modulate the activity of
10 class D β -lactamases and interfere with the post-translational carboxylation of Lys70. *Biochem J*
11 **2010**, 432, 495-504.
12
13

14
15
16
17 27. Bou, G.; Oliver, A.; Martinez-Beltran, J. OXA-24, a novel class D β -lactamase with
18 carbapenemase activity in an *Acinetobacter baumannii* clinical strain. *Antimicrob Agents*
19 *Chemother* **2000**, 44, 1556-1561.
20
21
22

23
24 28. Winkler, M. L.; Papp-Wallace, K. M.; Hujer, A. M.; Domitrovic, T. N.; Hujer, K. M.;
25 Hurless, K. N.; Tuohy, M.; Hall, G.; Bonomo, R. A. Unexpected challenges in treating
26 multidrug-resistant Gram-negative bacteria: resistance to ceftazidime-avibactam in archived
27 isolates of *Pseudomonas aeruginosa*. *Antimicrob Agents Chemother* **2015**, 59, 1020-1029.
28
29
30
31

32
33 29. Takalkar, S. S.; Chavan, R. P.; Patel, A. M.; Umalkar, K. V.; Satav, J. S.; Udaykar, A. P.;
34 Kulkarni, A. M.; Zope, V. S.; Bhagwat, S. S.; Patel, M. V. Sunday 441: WCK 5222 [Cefepime
35 (FEP)-WCK 5107 (Zidebactam, ZID)]: Thigh and lung PK/PD studies against higher MIC OXA
36 carbapenamase-expressing *A. baumannii*. In *ASM Microbe*, Boston, MA, 2016.
37
38
39
40

41
42 30. Joshi, P. R.; Khande, H. N.; Takalkar, S. S.; Kulkarni, A. M.; Chavan, R. P.; Zope, V. S.;
43 Palwe, S. R.; Biniwale, S. S.; Bhagwat, S. S.; Patel, M. V. Sunday 440: WCK 5222 [cefepime
44 (FEP)-WCK 5107 (zidebactam, ZID)]: *in vitro* and *in vivo* coverage of OXA-carbapenemases
45 expressing-*Acinetobacter*. In *ASM Microbe*, Boston, MA, 2016.
46
47
48
49

50
51 31. Khande, H. N.; Takalkar, S. S.; Umalkar, K. V.; Kulkarni, A. M.; Joshi, P. R.; Palwe, S.
52 R.; Biniwale, S. S.; Bhagwat, S. S.; Patel, M. V. Monday 424: WCK 5999 (carbapenem-WCK
53
54
55
56

1
2
3 4234): *in vitro* and *in vivo* activity of novel broader-spectrum β -lactam- β -lactamase inhibitor
4 against Indian OXA carbapenemase expressing *Acinetobacter*. In *ASM Microbe*, Boston, MA,
5
6 2016.
7

8
9
10 32. Bhagwat, S. S.; Takalkar, S. S.; Chavan, R. P.; Friedland, H. D.; Patel, M. V. Saturday
11
12 282: WCK 5222 [cefepime (FEP)-WCK 5107 (zidebactam, ZID)]: unravelling sub-MIC PD
13
14 effects employing *in vivo* dose fractionation studies and translating into MIC based PK/PD target
15
16 for carbapenem-resistant *A. baumannii*. In *ASM Microbe*, New Orleans, LA, 2017.
17

18
19 33. Bhagwat, S. S.; Takalkar, S. S.; Chavan, R. P.; Friedland, H. D.; Patel, M. V. Saturday
20
21 284: WCK 5222 [cefepime (FEP) + WCK 5107 (zidebactam, ZID)]: *in vivo* demonstration of
22
23 ZID-mediated β -lactam enhancer effect leading to lowering of FEP %f T>MIC against *P.*
24
25 *aeruginosa* and *A. baumannii*. In *ASM Microbe*, New Orleans, LA, 2017.
26

27
28 34. Patil, V. J.; Ravikumar, T.; Birajdar, S.; Bhagwat, S. Nitrogen Containing Compounds
29
30 and Their Use. WO2013038330A1, 2013.
31

32
33 35. Che, T.; Bethel, C. R.; Pusztai-Carey, M.; Bonomo, R. A.; Carey, P. R. The different
34
35 inhibition mechanisms of OXA-1 and OXA-24 β -lactamases are determined by the stability of
36
37 active site carboxylated lysine. *J Biol Chem* **2014**, *289*, 6152-6164.
38

39
40 36. Drawz, S. M.; Taracila, M.; Caselli, E.; Prati, F.; Bonomo, R. A. Exploring sequence
41
42 requirements for C(3)/C(4) carboxylate recognition in the *Pseudomonas aeruginosa*
43
44 cephalosporinase: Insights into plasticity of the AmpC β -lactamase. *Protein Sci* **2011**, *20*, 941-
45
46 958.
47

48
49 37. Hujer, K. M.; Hamza, N. S.; Hujer, A. M.; Perez, F.; Helfand, M. S.; Bethel, C. R.;
50
51 Thomson, J. M.; Anderson, V. E.; Barlow, M.; Rice, L. B.; Tenover, F. C.; Bonomo, R. A.
52
53 Identification of a new allelic variant of the *Acinetobacter baumannii* cephalosporinase, ADC-7
54
55

1
2
3 β -lactamase: defining a unique family of class C enzymes. *Antimicrob Agents Chemother* **2005**,
4
5
6 49, 2941-2948.

7
8 38. Knight, D.; Dimitrova, D. D.; Rudin, S. D.; Bonomo, R. A.; Rather, P. N. Mutations
9
10 decreasing intrinsic β -lactam resistance are linked to cell division in the nosocomial pathogen
11
12 *Acinetobacter baumannii*. *Antimicrob Agents Chemother* **2016**, 60, 3751-3758.

13
14
15 39. Leonard, D. A.; Hujer, A. M.; Smith, B. A.; Schneider, K. D.; Bethel, C. R.; Hujer, K.
16
17 M.; Bonomo, R. A. The role of OXA-1 β -lactamase Asp(66) in the stabilization of the active-site
18
19 carbamate group and in substrate turnover. *Biochem J* **2008**, 410, 455-462.

20
21
22 40. Ke, W.; Bethel, C. R.; Papp-Wallace, K. M.; Pagadala, S. R.; Nottingham, M.;
23
24 Fernandez, D.; Buynak, J. D.; Bonomo, R. A.; van den Akker, F. Crystal structures of KPC-2 β -
25
26 lactamase in complex with 3-nitrophenyl boronic acid and the penam sulfone PSR-3-226.
27
28 *Antimicrob Agents Chemother* **2012**, 56, 2713-2718.

29
30
31 41. Ke, W.; Bethel, C. R.; Thomson, J. M.; Bonomo, R. A.; van den Akker, F. Crystal
32
33 structure of KPC-2: insights into carbapenemase activity in class A β -lactamases. *Biochemistry*
34
35 **2007**, 46, 5732-5740.

36
37
38 42. Gonzalez, A., Tsay, Y. A Quick XDS Tutorial for SSRL.
39
40 http://smb.slac.stanford.edu/facilities/software/xds/#autoxds_script January 1, 2016.

41
42
43 43. Kabsch, W. Xds. *Acta Crystallogr D Biol Crystallogr* **2010**, 66, 125-132.

44
45 44. Murshudov, G. N.; Vagin, A. A.; Dodson, E. J. Refinement of macromolecular structures
46
47 by the maximum-likelihood method. *Acta Crystallogr D Biol Crystallogr* **1997**, 53, 240-255.

48
49
50 45. Emsley, P.; Cowtan, K. Coot: model-building tools for molecular graphics. *Acta*
51
52 *Crystallogr D Biol Crystallogr* **2004**, 60, 2126-2132.

- 1
2
3 46. Schuttelkopf, A. W.; van Aalten, D. M. PRODRG: a tool for high-throughput
4 crystallography of protein-ligand complexes. *Acta Crystallogr D Biol Crystallogr* **2004**, *60*,
5 1355-1363.
6
7
8
9
10 47. Laskowski, R. A.; MacArthur, M. W.; Moss, D. S.; Thornton, J. M. PROCHECK - a
11 program to check the stereochemical quality of protein structures. *J Appl Cryst* **2001**, *26*, 283-
12 291.
13
14
15
16
17 48. Wu, G.; Robertson, D. H.; Brooks, C. L. r.; Vieth, M. Detailed analysis of grid-based
18 molecular docking: A case study of CDOCKER-A CHARMM-based MD docking algorithm. *J*
19 *Comput Chem* **2003**, *24*, 1549-1562.
20
21
22
23
24 49. Drawz, S. M.; Taracila, M.; Caselli, E.; Prati, F.; Bonomo, R. A. Exploring sequence
25 requirements for C3/C4 carboxylate recognition in the *Pseudomonas aeruginosa*
26 cephalosporinase: Insights into plasticity of the AmpC β -Lactamase. *Protein Sci* **2011**, *20*, 941-
27 958.
28
29
30
31
32
33 50. Hori, T.; Nakano, M.; Kimura, Y.; Murakami, K. Pharmacokinetics and tissue
34 penetration of a new carbapenem, doripenem, intravenously administered to laboratory animals.
35 *In Vivo* **2006**, *20*, 91-96.
36
37
38
39
40
41
42
43
44
45
46
47
48
49
50
51
52
53
54
55
56
57
58
59
60

Table 1. Kinetic parameters

KPC-2	$K_{i\text{ app}} (\mu\text{M})$	$k_2/K (\text{M}^{-1}\text{s}^{-1})$	$k_{\text{off}} (\text{s}^{-1})$	Half-life (min)	$K_d (\text{nM})$	$k_{\text{cat}}/k_{\text{inact}}$
3	0.32 ± 0.03	$2.4 \pm 0.9 \times 10^5$	$4.5 \pm 0.5 \times 10^{-4}$	26 ± 3	1.9 ± 0.2	1
2	4.5 ± 0.5	$9.4 \pm 0.6 \times 10^3$	$4.0 \pm 0.4 \times 10^{-4}$	29 ± 3	43 ± 5	1
1	7.8 ± 0.8	$8.8 \pm 0.9 \times 10^3$	$3.5 \pm 0.5 \times 10^{-4}$	33 ± 5	40 ± 7	1
Avibactam	0.9 ± 0.1	1.3×10^{4a}	1.4×10^{-4a}	82^a	11^a	1
Relebactam	2.2 ± 0.3	$2.8 \pm 0.3 \times 10^4$	$2.5 \pm 0.5 \times 10^{-4}$	46 ± 9	9 ± 2	1
ADC-7						
ADC-7	$K_{i\text{ app}} (\mu\text{M})$	$k_2/K (\text{M}^{-1}\text{s}^{-1})$	$k_{\text{off}} (\text{s}^{-1})$	Half-life (min)	$K_d (\text{nM})$	$k_{\text{cat}}/k_{\text{inact}}$
3	8.0 ± 0.8	$1.9 \pm 0.2 \times 10^4$	$1.0 \pm 0.1 \times 10^{-3}$	12 ± 2	53 ± 7	6
2	2.3 ± 0.3	$3.5 \pm 0.4 \times 10^4$	$1.1 \pm 0.1 \times 10^{-3}$	11 ± 1	32 ± 3	4
1	3.7 ± 0.4	$3.2 \pm 0.3 \times 10^4$	$9.0 \pm 0.1 \times 10^{-4}$	13 ± 1	29 ± 3	4
Avibactam	19 ± 2	$3.9 \pm 0.4 \times 10^3$	$3.5 \pm 0.5 \times 10^{-4}$	33 ± 5	90 ± 9	4
Relebactam	12.6 ± 2	$7.8 \pm 0.8 \times 10^3$	$3.0 \pm 0.3 \times 10^{-4}$	39 ± 4	39 ± 4	2
PDC-3						
PDC-3	$K_{i\text{ app}} (\mu\text{M})$	$k_2/K (\text{M}^{-1}\text{s}^{-1})$	$k_{\text{off}} (\text{s}^{-1})$	Half-life (min)	$K_d (\text{nM})$	$k_{\text{cat}}/k_{\text{inact}}$
3	3.8 ± 0.4	$2.3 \pm 0.2 \times 10^4$	$2.8 \pm 0.3 \times 10^{-3}$	4.1 ± 0.4	124 ± 18	5
2	0.14 ± 0.01	$4.8 \pm 0.7 \times 10^5$	$3.5 \pm 0.4 \times 10^{-3}$	3.3 ± 0.4	7.3 ± 1.4	1
1	0.13 ± 0.02	$6.3 \pm 0.6 \times 10^5$	$4.0 \pm 0.4 \times 10^{-3}$	2.9 ± 0.3	6.3 ± 0.9	1
Avibactam	2.5 ± 0.3^a	2.9×10^{4a}	8×10^{-4a}	14.4^a	27.6^a	1
Relebactam	3.2 ± 0.3	$4.6 \pm 0.5 \times 10^4$	$9.0 \pm 0.1 \times 10^{-4}$	12.8 ± 1.4	20 ± 3	1
OXA-23						
OXA-23	$K_{i\text{ app}} (\mu\text{M})$	$k_2/K (\text{M}^{-1}\text{s}^{-1})$	$k_{\text{off}} (\text{s}^{-1})$	Half-life (min)	$K_d (\text{nM})$	$k_{\text{cat}}/k_{\text{inact}}$
3	8 ± 1	$1.7 \pm 0.2 \times 10^4$	$5.0 \pm 0.5 \times 10^{-4}$	23 ± 2	29 ± 4	1
2	> 100	ND	ND	ND	ND	ND

1	> 100	ND	ND	ND	ND	ND
Avibactam	> 100	3 x 10 ^{2a}	8.0 x 10 ^{-6a}	1,436 ^a	27 ^a	ND
Relebactam	> 100	ND	ND	ND	ND	ND
OXA-24/40	$K_{i\text{ app}} (\mu\text{M})$	$k_2/K (\text{M}^{-1}\text{s}^{-1})$	$k_{\text{off}} (\text{s}^{-1})$	Half-life (min)	K_d (nM)	$k_{\text{cat}}/k_{\text{inact}}$
3	5.0 ± 0.5	9.6 ± 1.0 x 10 ³	4.0 ± 0.4 x 10 ⁻⁴	29 ± 3	42 ± 6	2
2	> 100	ND	ND	ND	ND	ND
1	> 100	ND	ND	ND	ND	ND
Avibactam	> 100	5.2 x 10 ^{1a}	6.3 x 10 ^{-6a}	1,823 ^a	121 ^a	ND
Relebactam	> 100	ND	ND	ND	ND	ND
OXA-48	$K_{i\text{ app}} (\mu\text{M})$	$k_2/K (\text{M}^{-1}\text{s}^{-1})$	$k_{\text{off}} (\text{s}^{-1})$	Half-life (min)	K_d (nM)	$k_{\text{cat}}/k_{\text{inact}}$
3	0.29 ± 0.03	6.4 ± 0.6 x 10 ⁵	9.0 ± 0.1 x 10 ⁻⁴	13 ± 1	1.4 ± 0.2	2
2	> 100	ND	ND	ND	ND	ND
1	> 100	ND	ND	ND	ND	ND
Avibactam	30 ± 3	1.4 x 10 ^{3a}	1.2 ± x 10 ^{-5a}	1,000 ^a	9 ^a	1
Relebactam	> 100	ND	ND	ND	ND	ND

^aPreviously published data^{4,5}. ND, if $K_{i\text{ app}}$ values were >100 μM then further kinetic analyses were not determined.

Table 2. Mass spectrometry data for β -lactamases incubated with DBOs for 5 min and 24 hr.

Sample	Inhibitor	5 min		24 hr	
		Molecular weight (MW)	Δ MW (Δ DBO)	MW	Δ MW (Δ DBO)
KPC-2	None	28,723	+0	28,724	+0
KPC-2	3	28,971	+247	28,971	+247
KPC-2	2	29,115	+392	29,115	+392
KPC-2	1	29,101	+378	29,101	+378
KPC-2	Avibactam	28,989	+266	28,989 28,892	+265 +168 (-97)
KPC-2	Relebactam	29,071	+349	29,072	+350
ADC-7					
ADC-7	None	40,639	+0	40,640	+0
ADC-7	3	40,639 (minor) 40,886 40,806 (minor)	+0 +248 +166 (-80)	40,640 40,887 40,806 (minor)	+0 +247 +166 (-80)
ADC-7	2	40,639 (minor) 41,030	+0 +391	40,640 41,031 (minor)	+0 +247
ADC-7	1	40,639 41,016	+0 +377	40,640 41,018 (minor)	+0 +377
ADC-7	Avibactam	40,640 (minor) 40,904 40,824 (minor)	+0 +264 +185 (-80)	40,641 40,905 40,824	+0 +264 +185 (-80)
ADC-7	Relebactam	40,639 (minor) 40,987	+0 +349	40,989	+348
PDC-3					
PDC-3	None	40,654 40,785	+0 +0	40,655 40,786	+0 +0

1	PDC-3	3	41,033	+246	41,033	+246
2			40,902	+246	40,903	+246
3			40,951 (minor)	+166 (-80)	40,951 (minor)	+166 (-80)
4			40,820 (minor)	+166 (-80)	40,822 (minor)	+166 (-80)
5						
6	PDC-3	2	41,177	+394	41,178	+394
7			41,046	+394	41,046	+394
8						
9	PDC-3	1	41,163	+383	41,163	+383
10			41,032	+383	41,032	+383
11						
12	PDC-3	Avibactam	41,051	+265	41,051	+265
13			40,920	+265	40,920	+265
14			40,970 (minor)	+185 (-80)	40,970 (minor)	+185 (-80)
15			40,840 (minor)	+185 (-80)	40,840 (minor)	+185 (-80)
16						
17	PDC-3	Relebactam	41,134	+353	41,134	+353
18			41,003	+353	41,004	+353
19						
20						
21	OXA-23	None	27,494	+0	27,494	+0
22						
23	OXA-23	3	27,494 (minor)	+0	27,494 (minor)	+0
24			27,740	+246	27,741	+247
25			27,660 (minor)	+166 (-80)	27,660 (minor)	+167 (-80)
26						
27						
28	OXA-24/40	None	28,664	+0	28,664	+0
29						
30	OXA-24/40	3	28,664 (minor)	+0	28,665 (minor)	+0
31			28,911	+247	28,912	+247
32			288,32 (minor)	+166 (-80)	28,832 (minor)	+166 (-80)
33						
34						
35	OXA-48	None	28,283	+0	28,290	+0
36						
37	OXA-48	3	28,283 (minor)	+0	28,286 (minor)	+0
38			28,530	+247	28,533	+247
39			28,449 (minor)	+166 (-80)	28,451 (minor)	+166 (-80)
40						
41	OXA-48	Avibactam	28,549	+266	28,551	+265
42			28,468 (minor)	+185 (-80)		
43						

Table 3. Susceptibility testing results for DBOs alone and in combination with cefepime or meropenem.

STRAIN	3	2	1	Avibactam	Relebactam	Cefepime	Cefepime/3-4 ^a	Cefepime/3-8 ^a	Cefepime/1-4	Cefepime/1-8	Cefepime/2-4	Cefepime/2-8	Cefepime/Avibactam-4	Cefepime/Relebactam-4	Meropenem	Meropenem/3-4	Meropenem/3-8	Meropenem/1-4	Meropenem/1-8	Meropenem/2-4	Meropenem/2-8	Meropenem/Avibactam-4	Meropenem/Relebactam-4
Isogenic strains																							
<i>Escherichia coli</i> DH10B (Control)	> 16	≤ 0.12	≤ 0.12	16	> 16	≤ 0.12	≤ 0.12	≤ 0.12	≤ 0.12	≤ 0.12	≤ 0.12	≤ 0.12	≤ 0.12	≤ 0.12	≤ 0.12	≤ 0.12	≤ 0.12	≤ 0.12	≤ 0.12	≤ 0.12	≤ 0.12	≤ 0.12	≤ 0.12
<i>E. coli</i> DH10B pBR322-catI-KPC-2	> 16	0.25	0.25	> 16	> 16	> 16	≤ 0.12	≤ 0.12	≤ 0.12	≤ 0.12	≤ 0.12	≤ 0.12	≤ 0.12	≤ 0.12	8	≤ 0.12	≤ 0.12	≤ 0.12	≤ 0.12	≤ 0.12	≤ 0.12	≤ 0.12	≤ 0.12
<i>E. coli</i> DH10B pBC SK(-) KPC-2	> 16	≤ 0.12	≤ 0.12	> 16	> 16	0.5	≤ 0.12	≤ 0.12	≤ 0.12	≤ 0.12	≤ 0.12	≤ 0.12	≤ 0.12	≤ 0.12	≤ 0.12	≤ 0.12	≤ 0.12	≤ 0.12	≤ 0.12	≤ 0.12	≤ 0.12	≤ 0.12	≤ 0.12
<i>E. coli</i> DH10B pBC SK(-) KPC-3	> 16	≤ 0.12	0.25	> 16	> 16	2	≤ 0.12	≤ 0.12	≤ 0.12	≤ 0.12	≤ 0.12	≤ 0.12	≤ 0.12	≤ 0.12	0.5	≤ 0.12	≤ 0.12	≤ 0.12	≤ 0.12	≤ 0.12	≤ 0.12	≤ 0.12	≤ 0.12
<i>E. coli</i> DH10B pBC SK(-) PDC-3	> 16	≤ 0.12	0.25	16	> 16	≤ 0.12	≤ 0.12	≤ 0.12	≤ 0.12	≤ 0.12	≤ 0.12	≤ 0.12	≤ 0.12	≤ 0.12	≤ 0.12	≤ 0.12	≤ 0.12	≤ 0.12	≤ 0.12	≤ 0.12	≤ 0.12	≤ 0.12	≤ 0.12
<i>E. coli</i> DH10B pBC SK(-) OXA-48	> 16	≤ 0.12	≤ 0.12	16	> 16	≤ 0.12	≤ 0.12	≤ 0.12	≤ 0.12	≤ 0.12	≤ 0.12	≤ 0.12	≤ 0.12	≤ 0.12	0.25	≤ 0.12	≤ 0.12	≤ 0.12	≤ 0.12	≤ 0.12	≤ 0.12	≤ 0.12	0.25
<i>A. baumannii</i> ΔADC	> 16	> 16	> 16	> 16	> 16	0.25	0.5	0.5	0.5	0.5	0.25	0.5	0.5	0.25	≤ 0.12	≤ 0.12	≤ 0.12	≤ 0.12	≤ 0.12	≤ 0.12	≤ 0.12	≤ 0.12	≤ 0.12
<i>A. baumannii</i> ΔADC pWH1266 OXA-23	> 16	> 16	> 16	> 16	> 16	> 16	2	2	16	16	16	16	> 16	> 16	> 16	16	4	> 16	> 16	> 16	> 16	> 16	> 16
<i>A. baumannii</i> ΔADC pWH1266 OXA-24/40	> 16	> 16	> 16	> 16	> 16	> 16	16	16	16	16	16	16	> 16	> 16	> 16	> 16	> 16	> 16	> 16	> 16	> 16	> 16	> 16
Clinical <i>K. pneumoniae</i> isolates producing bla_{KPC} – Colistin Resistant (CoIR) and colistin susceptible (CoIS)																							
<i>K. pneumoniae</i> 660/1568 CoIR KPC-3	> 16	≤ 0.12	≤ 0.12	4	> 16	16	0.25	0.25	≤ 0.12	≤ 0.12	≤ 0.12	≤ 0.12	≤ 0.12	0.25	2	≤ 0.12	≤ 0.12	≤ 0.12	≤ 0.12	≤ 0.12	≤ 0.12	≤ 0.12	≤ 0.12
<i>K. pneumoniae</i> 729/1679 CoIR KPC-2	> 16	2	0.5	> 16	> 16	> 16	0.5	0.25	≤ 0.12	≤ 0.12	≤ 0.12	≤ 0.12	0.25	0.5	> 16	≤ 0.12	≤ 0.12	≤ 0.12	≤ 0.12	≤ 0.12	≤ 0.12	≤ 0.12	≤ 0.12
<i>K. pneumoniae</i> 776/1742 CoIR KPC-2	> 16	0.5	0.5	> 16	> 16	> 16	1	1	≤ 0.12	≤ 0.12	≤ 0.12	≤ 0.12	0.5	1	> 16	0.5	0.25	0.25	≤ 0.12	≤ 0.12	≤ 0.12	≤ 0.12	0.5
<i>K. pneumoniae</i> 901/1860 CoIR KPC-3	> 16	> 16	> 16	> 16	> 16	16	≤ 0.12	≤ 0.12	≤ 0.12	≤ 0.12	≤ 0.12	≤ 0.12	≤ 0.12	≤ 0.12	16	≤ 0.12	≤ 0.12	≤ 0.12	≤ 0.12	≤ 0.12	≤ 0.12	≤ 0.12	≤ 0.12
<i>K. pneumoniae</i> 935/1884 CoIR KPC-3	> 16	> 16	> 16	> 16	> 16	> 16	0.25	≤ 0.12	≤ 0.12	≤ 0.12	≤ 0.12	≤ 0.12	≤ 0.12	≤ 0.12	> 16	≤ 0.12	≤ 0.12	≤ 0.12	≤ 0.12	≤ 0.12	≤ 0.12	≤ 0.12	≤ 0.12
<i>K. pneumoniae</i> 977/1916 CoIR KPC-3	> 16	> 16	2	> 16	> 16	16	≤ 0.12	≤ 0.12	≤ 0.12	≤ 0.12	≤ 0.12	≤ 0.12	≤ 0.12	0.25	> 16	≤ 0.12	≤ 0.12	≤ 0.12	≤ 0.12	≤ 0.12	≤ 0.12	≤ 0.12	≤ 0.12
<i>K. pneumoniae</i> 1084/1957 CoIR KPC-3	> 16	> 16	> 16	> 16	> 16	> 16	≤ 0.12	≤ 0.12	≤ 0.12	≤ 0.12	≤ 0.12	≤ 0.12	≤ 0.12	0.25	16	≤ 0.12	≤ 0.12	≤ 0.12	≤ 0.12	≤ 0.12	≤ 0.12	≤ 0.12	≤ 0.12
<i>K. pneumoniae</i> 1108/1989 CoIR KPC-3	> 16	> 16	> 16	> 16	> 16	> 16	0.25	≤ 0.12	≤ 0.12	≤ 0.12	≤ 0.12	≤ 0.12	≤ 0.12	0.5	> 16	≤ 0.12	≤ 0.12	≤ 0.12	≤ 0.12	≤ 0.12	≤ 0.12	≤ 0.12	≤ 0.12

<i>K. pneumoniae</i> 1315/2198 ColR KPC-3	> 16	<= 0.12	<= 0.12	4	> 16	> 16	0.25	0.25	<= 0.12	<= 0.12	<= 0.12	<= 0.12	<= 0.12	0.25	> 16	<= 0.12	<= 0.12	<= 0.12	<= 0.12	<= 0.12	<= 0.12	<= 0.12	<= 0.12	<= 0.12
<i>K. pneumoniae</i> 1398/2291 ColR KPC-3	> 16	1	2	> 16	> 16	> 16	<= 0.12	0.25	<= 0.12	<= 0.12	<= 0.12	<= 0.12	<= 0.12	<= 0.12	16	<= 0.12	<= 0.12	<= 0.12	<= 0.12	<= 0.12	<= 0.12	<= 0.12	<= 0.12	<= 0.12
<i>K. pneumoniae</i> 761/1723 ColS KPC-3	> 16	<= 0.12	<= 0.12	16	> 16	8	<= 0.12	<= 0.12	<= 0.12	<= 0.12	<= 0.12	<= 0.12	<= 0.12	<= 0.12	16	<= 0.12	<= 0.12	<= 0.12	<= 0.12	<= 0.12	<= 0.12	<= 0.12	<= 0.12	<= 0.12
<i>K. pneumoniae</i> 972/1910 ColS KPC-3	> 16	<= 0.12	<= 0.12	4	> 16	16	0.25	0.25	<= 0.12	<= 0.12	<= 0.12	<= 0.12	<= 0.12	0.25	8	<= 0.12	<= 0.12	<= 0.12	<= 0.12	<= 0.12	<= 0.12	<= 0.12	<= 0.12	<= 0.12
<i>K. pneumoniae</i> 1354/2241 ColS KPC-3	> 16	8	8	> 16	> 16	> 16	<= 0.12	<= 0.12	<= 0.12	<= 0.12	<= 0.12	<= 0.12	<= 0.12	<= 0.12	16	<= 0.12	<= 0.12	<= 0.12	<= 0.12	<= 0.12	<= 0.12	<= 0.12	<= 0.12	<= 0.12
<i>K. pneumoniae</i> 440/1360 ColS KPC-2	> 16	0.25	0.5	16	> 16	> 16	0.5	0.25	<= 0.12	<= 0.12	<= 0.12	<= 0.12	<= 0.12	1	> 16	<= 0.12	<= 0.12	<= 0.12	<= 0.12	<= 0.12	<= 0.12	<= 0.12	<= 0.12	<= 0.12

Clinical Enterobacteriaceae isolates producing *bla*_{OXA-48} and mutants

<i>K. pneumoniae</i> 11978 OXA-48	> 16	> 16	> 16	> 16	> 16	16	0.5	0.5	<= 0.12	<= 0.12	<= 0.12	<= 0.12	0.25	2	> 16	<= 0.12	<= 0.12	1	<= 0.12	<= 0.12	<= 0.12	1	> 16	
<i>K. pneumoniae</i> CAV 1636 OXA-181	> 16	> 16	8	> 16	> 16	> 16	0.5	0.5	<= 0.12	<= 0.12	<= 0.12	<= 0.12	0.5	4	> 16	<= 0.12	<= 0.12	<= 0.12	<= 0.12	1	<= 0.12	1	16	
<i>K. pneumoniae</i> CAV 1543 OXA-48	> 16	1	1	> 16	> 16	> 16	0.25	0.25	<= 0.12	<= 0.12	<= 0.12	<= 0.12	0.25	2	8	<= 0.12	<= 0.12	<= 0.12	<= 0.12	<= 0.12	<= 0.12	<= 0.12	8	
<i>K. pneumoniae</i> NY BS OXA-232	> 16	1	2	16	> 16	> 16	0.5	1	<= 0.12	<= 0.12	<= 0.12	<= 0.12	0.5	2	> 16	0.25	0.12	0.12	0.12	0.12	0.12	0.12	0.5	> 16
<i>K. pneumoniae</i> Jefferson 17,73 OXA-181	> 16	> 16	> 16	> 16	> 16	> 16	1	1	<= 0.12	<= 0.12	<= 0.12	<= 0.12	1	4	> 16	0.25	0.25	0.5	0.5	1	<= 0.12	1	16	
<i>E. coli</i> Jefferson 17,75 OXA-48	> 16	> 16	> 16	> 16	> 16	8	<= 0.12	<= 0.12	<= 0.12	<= 0.12	<= 0.12	<= 0.12	<= 0.12	0.25	2	<= 0.12	<= 0.12	<= 0.12	<= 0.12	<= 0.12	<= 0.12	<= 0.12	2	

Ceftazidime-avibactam-resistant clinical *P. aeruginosa* isolates²⁸

<i>P. aeruginosa</i> CL232	> 16	> 16	> 16	> 16	> 16	> 16	> 16	> 16	8	4	16	16	> 16	16	> 16	> 16	> 16	> 16	16	> 16	> 16	> 16	> 16
<i>P. aeruginosa</i> 715	> 16	> 16	16	> 16	> 16	> 16	16	> 16	8	0.25	8	16	16	16	> 16	> 16	16	16	0.5	16	8	16	16
<i>P. aeruginosa</i> 776	> 16	> 16	8	> 16	> 16	> 16	> 16	> 16	16	0.25	16	16	> 16	16	> 16	16	> 16	16	16	16	16	> 16	> 16
<i>P. aeruginosa</i> 795	> 16	16	4	> 16	> 16	> 16	> 16	> 16	0.5	<= 0.12	16	16	> 16	> 16	16	16	16	4	<= 0.12	16	4	16	8
<i>P. aeruginosa</i> 839	> 16	8	4	> 16	> 16	8	8	8	<= 0.12	<= 0.12	2	0.5	4	4	1	1	1	<= 0.12	<= 0.12	0.5	<= 0.12	1	1

Clinical *A. baumannii* isolates producing *bla*_{OXA-23} and/or *bla*_{OXA-24}

<i>A. baumannii</i> PR319 OXA-23 and OXA-24/40	> 16	> 16	> 16	> 16	> 16	> 16	> 16	> 16	> 16	> 16	> 16	> 16	> 16	> 16	> 16	> 16	> 16	> 16	> 16	> 16	> 16	> 16	> 16
<i>A. baumannii</i> PR323 OXA-24/40	> 16	> 16	> 16	> 16	> 16	> 16	> 16	> 16	4	8	4	4	> 16	> 16	> 16	16	16	> 16	> 16	> 16	> 16	> 16	> 16
<i>A. baumannii</i> PR359 OXA-23	> 16	> 16	> 16	> 16	> 16	16	8	8	8	16	8	16	16	16	> 16	4	4	> 16	> 16	> 16	> 16	> 16	> 16
<i>A. baumannii</i> PR363 OXA-23	> 16	> 16	> 16	> 16	> 16	16	8	8	8	8	8	8	> 16	16	> 16	4	2	> 16	> 16	> 16	> 16	> 16	> 16
<i>A. baumannii</i> PR381 OXA-24/40	> 16	> 16	> 16	> 16	> 16	> 16	16	16	16	16	16	16	> 16	> 16	> 16	> 16	> 16	> 16	> 16	> 16	> 16	> 16	> 16
<i>A. baumannii</i> PR408 OXA-24/40	> 16	> 16	> 16	> 16	> 16	16	8	8	16	16	8	16	> 16	16	> 16	> 16	> 16	> 16	> 16	> 16	> 16	> 16	> 16
<i>A. baumannii</i> PR420 OXA-23 and OXA-24/40	> 16	> 16	> 16	> 16	> 16	> 16	> 16	> 16	> 16	> 16	> 16	> 16	> 16	> 16	> 16	16	8	> 16	> 16	> 16	> 16	> 16	> 16
<i>A. baumannii</i> PR440	> 16	> 16	> 16	> 16	> 16	> 16	16	> 16	> 16	> 16	16	> 16	16	> 16	> 16	4	2	> 16	> 16	> 16	> 16	> 16	> 16

Table 4. *In vivo* efficacy of cefepime-2, meropenem-3, and comparators in peritonitis model.

Strains	β -lactamases	Infecting Load CFU/mouse	Treatment protocol	Antibiotics	MIC ($\mu\text{g/mL}$) ^a	PD ₅₀ (mg/kg)	PD ₉₀ (mg/kg)
<i>A. baumannii</i> NCTC 13301	OXA-23, OXA-51	3.5×10^5	+1hr PI, Two doses	cefepime	>256	>100	>100
				cefepime-2 ^b	16	100 + 23.23	100 + 52.30
		3.5×10^6	+1hr PI, Two doses	meropenem ^c	32	>100	>100
				meropenem-3	1	25 + 16.30	25 + 23.71
				tigecycline	1	>6.25	>6.25
				Three doses	colistin	1	16.57
<i>A. baumannii</i> NCTC 13303	OXA-26, OXA-51-like	2.5×10^6	+1hr PI, Two doses	cefepime	64	>200	>200
				cefepime-2	16	50 + < 23.23	50 + 23.23
		2.5×10^6	+2hr PI, Two doses	meropenem	256	>100	>100
				meropenem-3	16	50 + 24.01	50 + 49.38
				tigecycline	1	>6.25	>6.25
		Three doses	colistin	0.5	11.72	18.72	
<i>A. baumannii</i> SL46	OXA-23, OXA-51	3×10^6	+1hr PI, Two doses	cefepime	>512	>200	>200
				cefepime-2	32	50 + 23.23	100 + 52.30
		3×10^6	+2hr PI, Two doses	meropenem	64	>100	>100
				meropenem-3	8	50 + 24.91	50 + 66.17

^aFor MIC determinations, **3** was used at fixed 8 $\mu\text{g/mL}$ concentration. cefepime-2 MICs were determined at 1:1 ratio.

^b2 as a monotherapy at 200 mg/kg did not result into protection of infected animals.

^cMeropenem was administered in combination with cilastatin (1:1) due to meropenem's instability to murine renal DHP-1⁵⁰.

Abbreviations: PI: Post Infection; Two doses: the drugs were administered twice, 3 hr apart; Three doses: the drugs were administered thrice, 3 hr apart.

Figure Legends.

Figure 1. Structures of DBOs used in this study. R¹ side chain is highlighted by a dotted circle.

Figure 2. A. Synthesis of **1** and **2**. **B.** Synthesis of **3**.

Figure 3. A. Scheme representing the interactions of β -lactamases with DBOs. In this model, formation of the non-covalent complex, enzyme:inhibitor (E: I) is represented by the dissociation constant, K_d , which is equivalent to k_{-1}/k_1 . k_2 is the first order rate constant for the acylation step, or formation of E-I. k_{-2} is the first order rate constant for the recyclization step or re-formation of E:I. Reported rarely to date, some DBOs under a desulfation reaction, k_3 is the first order rate constant for desulfation to form E:I*, where I* is the desulfated DBO. The desulfated DBO may undergo complete hydrolysis; the hydrolysis, which forms free E and product (P) is represented by the first order rate constant k_4 . **B.** A chemical representation of the scheme panel A using avibactam. **C.** Acyl-transfer mass spectrometry with **3** (left), **2** (center), and **1** (right). Each DBO was preincubated with KPC-2 at a 1:1 E:I ratio for 1 min (data in top panels in blue) and used for mass spectrometry, then TEM-1 was added incubated for 15 sec or 5 min (data in center and bottom panels in red) and used for mass spectrometry.

Figure 4. A. Electron density of compounds **1**, **2**, and **3** bound in the active site of KPC-2. Shown are unbiased omit $|F_o|-|F_c|$ electron density with the ligand removed from refinement and map calculations. Left, **3** bound to KPC-2; center, **2** bound to KPC-2; right, **1** bound to KPC-2. Compounds **1**, **2**, and **3** are shown in blue carbon atom ball-and-stick representation whereas the protein is depicted in grey carbon atom stick representation. Electron density is contoured at 3σ level and data sets are from inhibitor soaked KPC-2 crystals. The sulfate moiety of **3** was observed to be in two conformations (0.6 and 0.4 occupancy conformations labeled a, and b, respectively). **B.** Compounds **1**, **2**, and **3** bound to the active site of KPC-2. Left, **3** bound to KPC-2; center, **2** bound to KPC-2; right, **1** bound to KPC-2. Hydrogen bonds are depicted as dashed lines; the distances for key hydrogen bonds are shown (in Å). The deacylation water molecule is labeled as W#1. The two conformations for the sulfate moiety in **3** is labeled similar as in panel A.

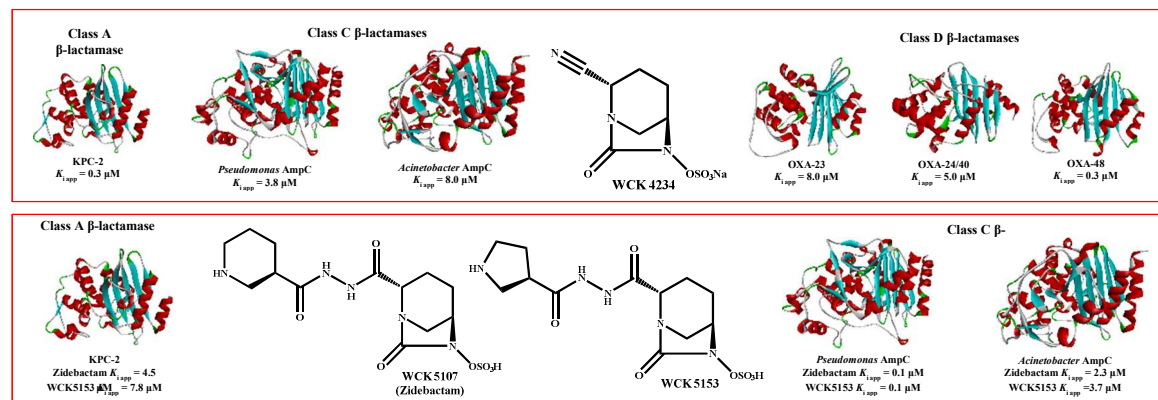
1 **Figure 5.** Stereo figure of superimpositioning of DBO inhibitors in active site of KPC-2. Depicted are **3** bound to KPC-2 molecule A (grey), **3** bound
2 to KPC-2 molecule B (light green), **2** bound to KPC-2 molecule A (blue), **1** bound to KPC-2 molecule A (gold), avibactam bound to KPC-2 molecule
35 A (dark green; PDBid: 4ZBE). Structures used for the superimposition are from inhibitor soaked KPC-2 crystals.
4
5
6
7

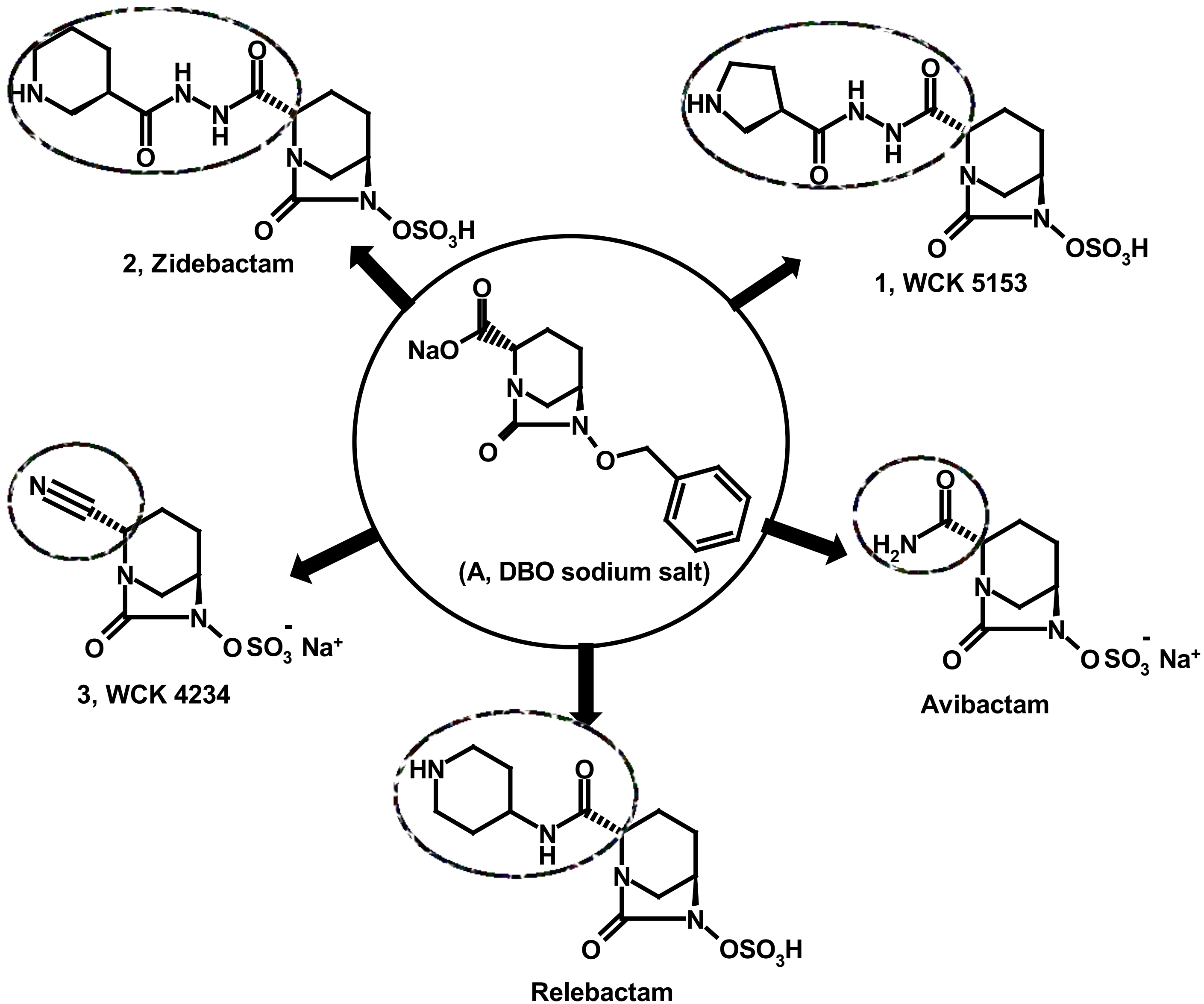
8 **Figure 6.** Compound **3** bound to OXA-24. **A.** Unbiased omit $|F_o|-|F_c|$ electron density of **3**:OXA-24 complex with the ligand removed from
9 refinement and map calculations. Density is contoured at 3σ level. **B.** Interactions of **3** in active site of OXA-24; the distances for key hydrogen
10 bonds are shown (in Å). **C.** Stereo figure depicting the superimpositioning of OXA-24 in complex with **3** (cyan **3** carbon atoms and grey protein
11 carbon atoms) and in complex with avibactam (blue carbon atoms for avibactam and protein; PDBid 4WM9). In close proximity to the **3** ligand, a
12 chloride ion in two alternate positions is present and labeled Cl1 and Cl2.
13
14
15
16
17

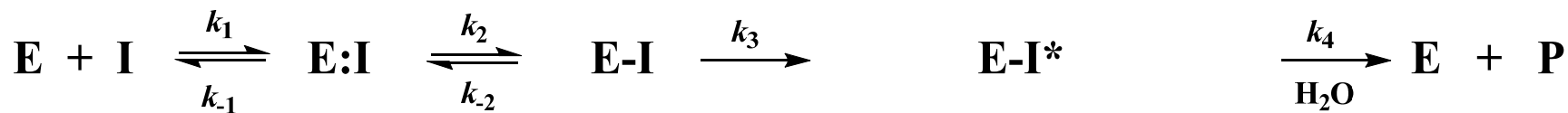
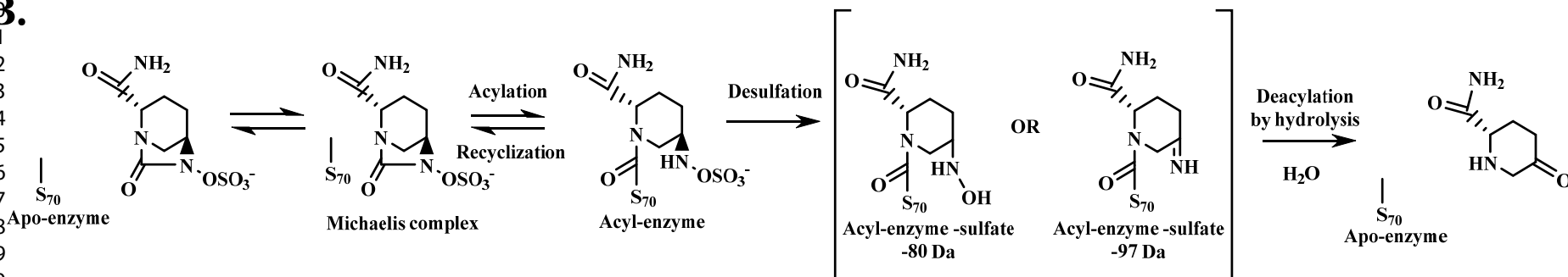
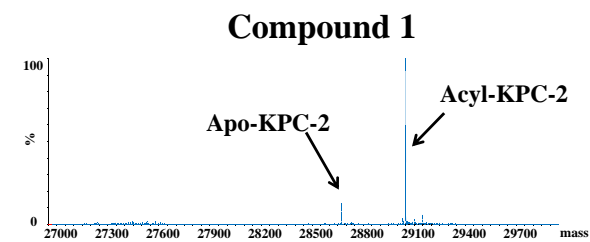
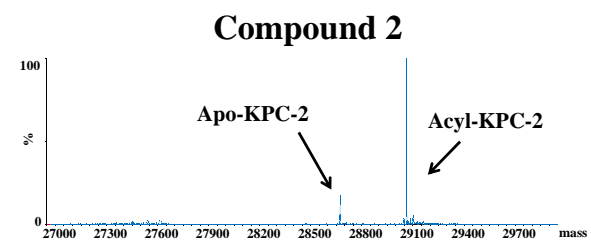
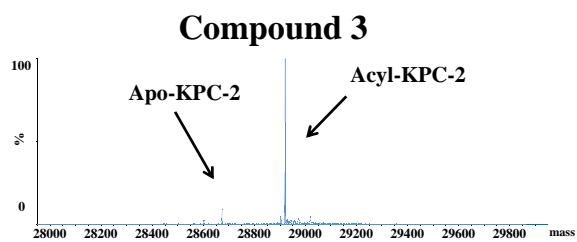
18 **Figure 7. A.** A murine neutropenic lung infection model using an Indian clinical isolate of *A. baumannii* SL06 carrying *bla*_{OXA-23} and *bla*_{OXA-51}. The
19 graphs represent the change in CFU/lung after different antibiotic treatments administered as q2h. A. Cefepime at 50 mg/kg (FEP),
20 meropenem:cilastatin at a 1:1 ratio of 25 mg/kg (MEM:CLS), and imipenem:cilastatin at a 1:1 ratio of 25 mg/kg (IPM:CLS). **B.** Cefepime-**2** at 50
21 mg/kg and 8.33 mg/kg, respectively (FEP-**2**), meropenem:cilastatin at a 1:1 ratio of 25 mg/kg and 4.68 mg/kg of **3** (MEM:CLS-**3**), and
22 imipenem:cilastatin at a 1:1 ratio of 25 mg/kg and 18.75 mg/kg of relebactam (IPM:CLS-REL).
23
24
25
26
27
28
29
30
31
32
33
34
35
36
37
38
39
40
41
42
43
44
45
46
47

1
2
3
4
5
6
7
8
9

Table of Contents Graphic.

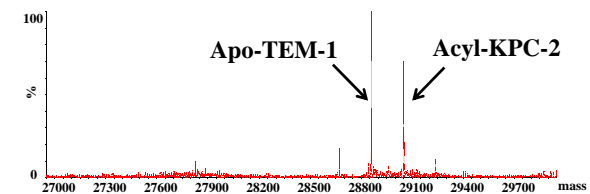
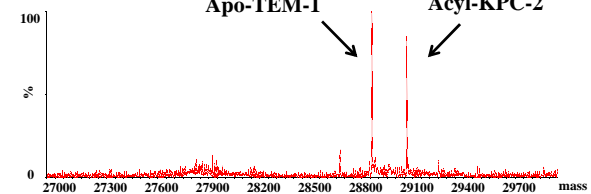
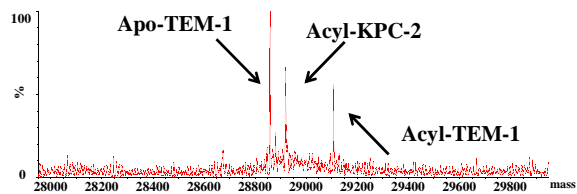




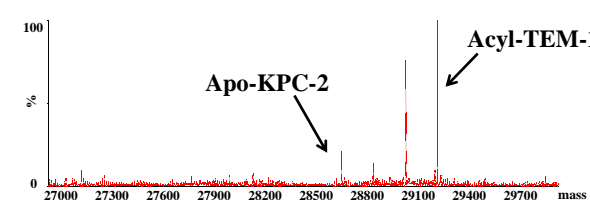
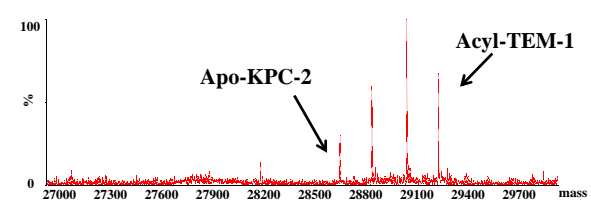
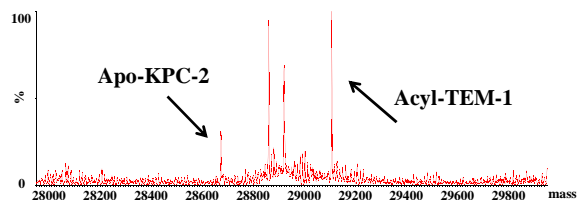
1
2
3
4
5
6
7
8
9
10
11
12
13
14
15
16
17
18
19
20
21
22
23
24
25
26
27
28
29
30
31
32
33
34
35
36
37
38
39
40
41
42
43
44
45
46
47**A.****B.****C.**1 min
preincubation

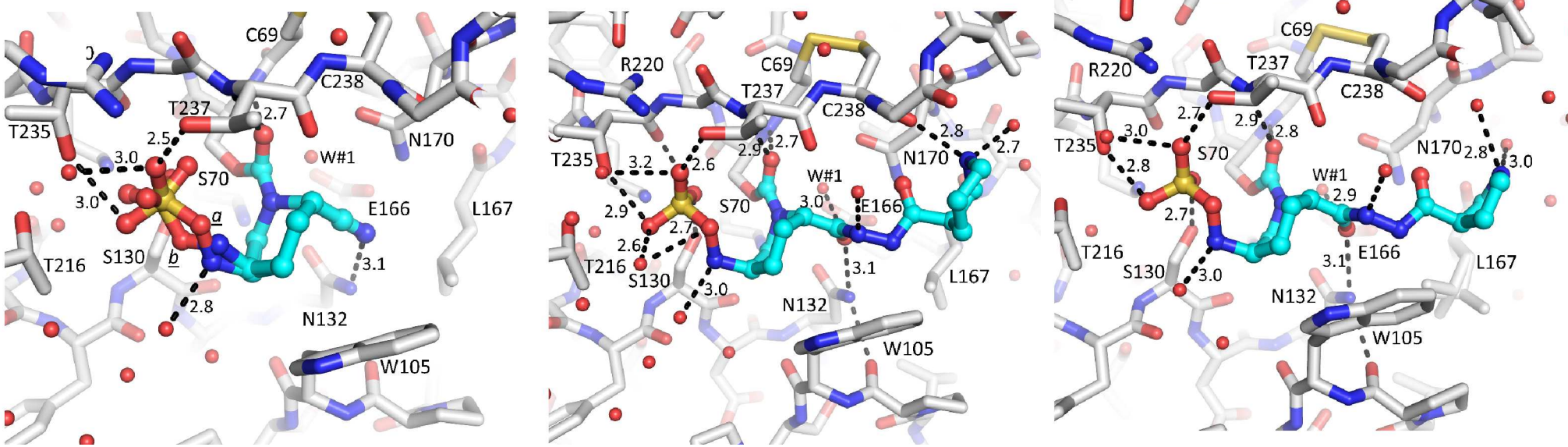
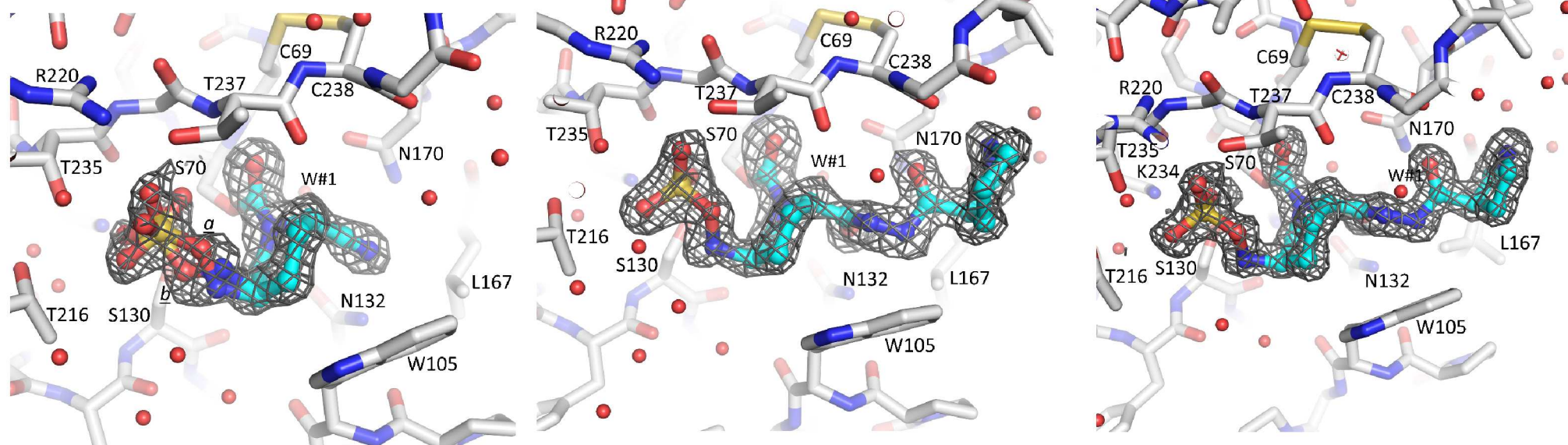
+ TEM-1

15 sec

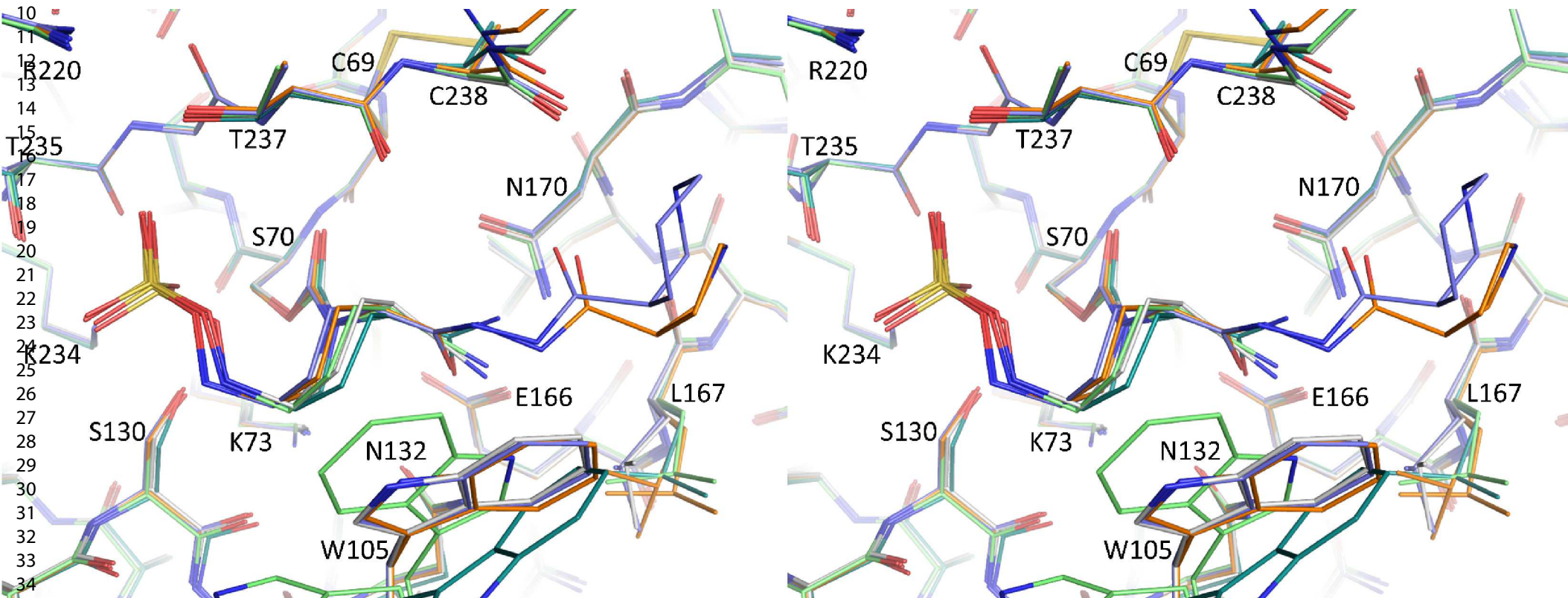


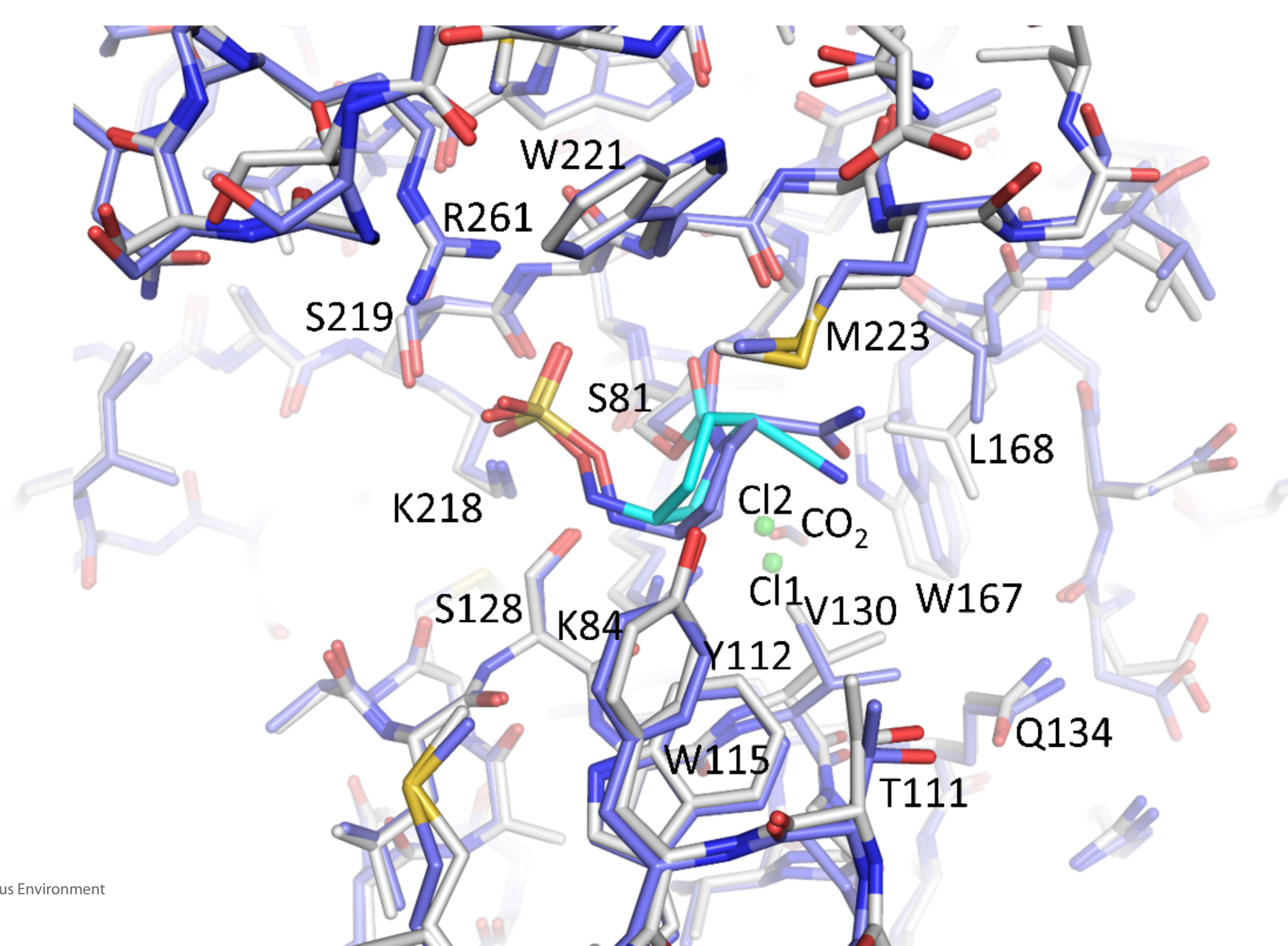
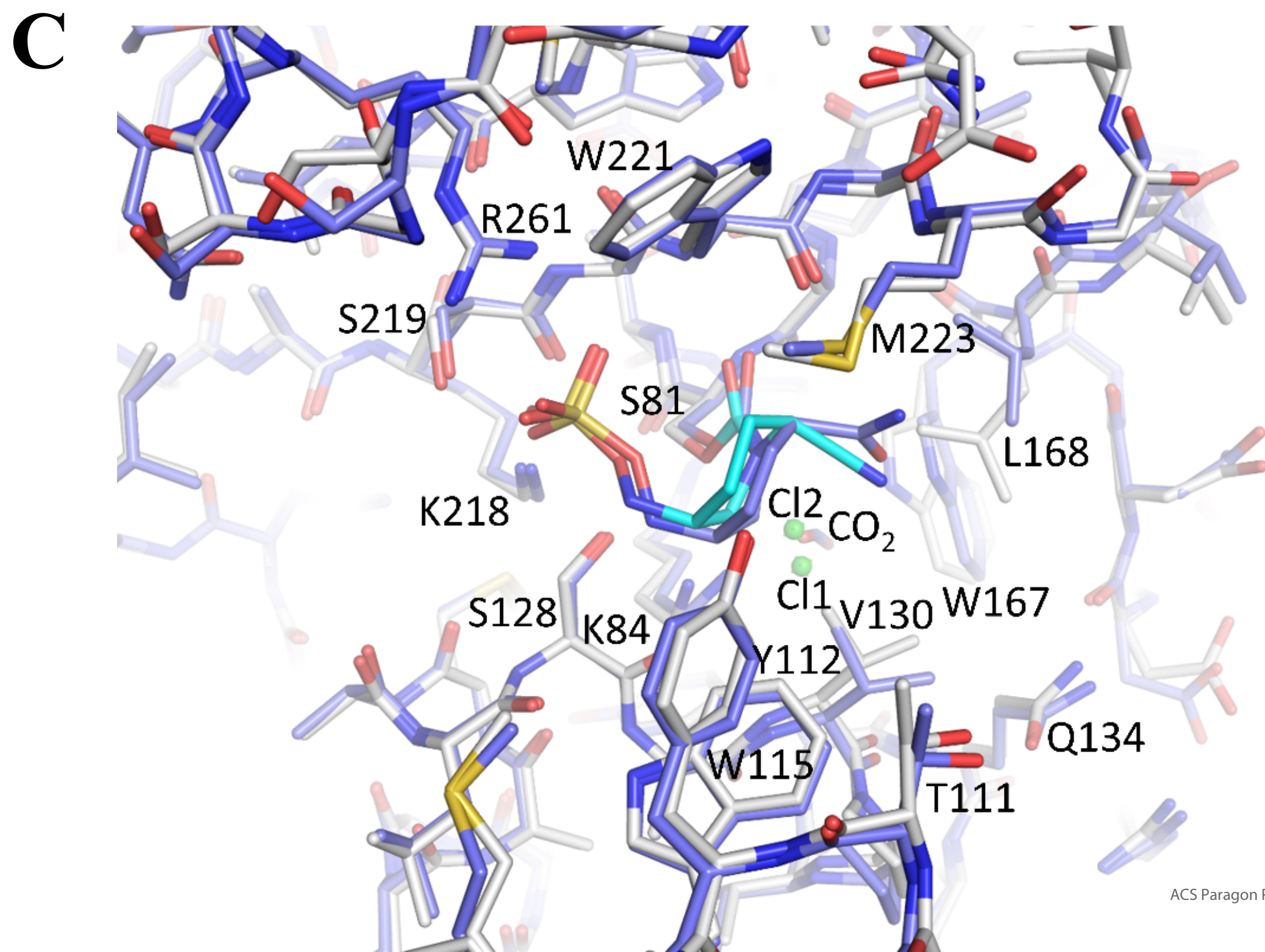
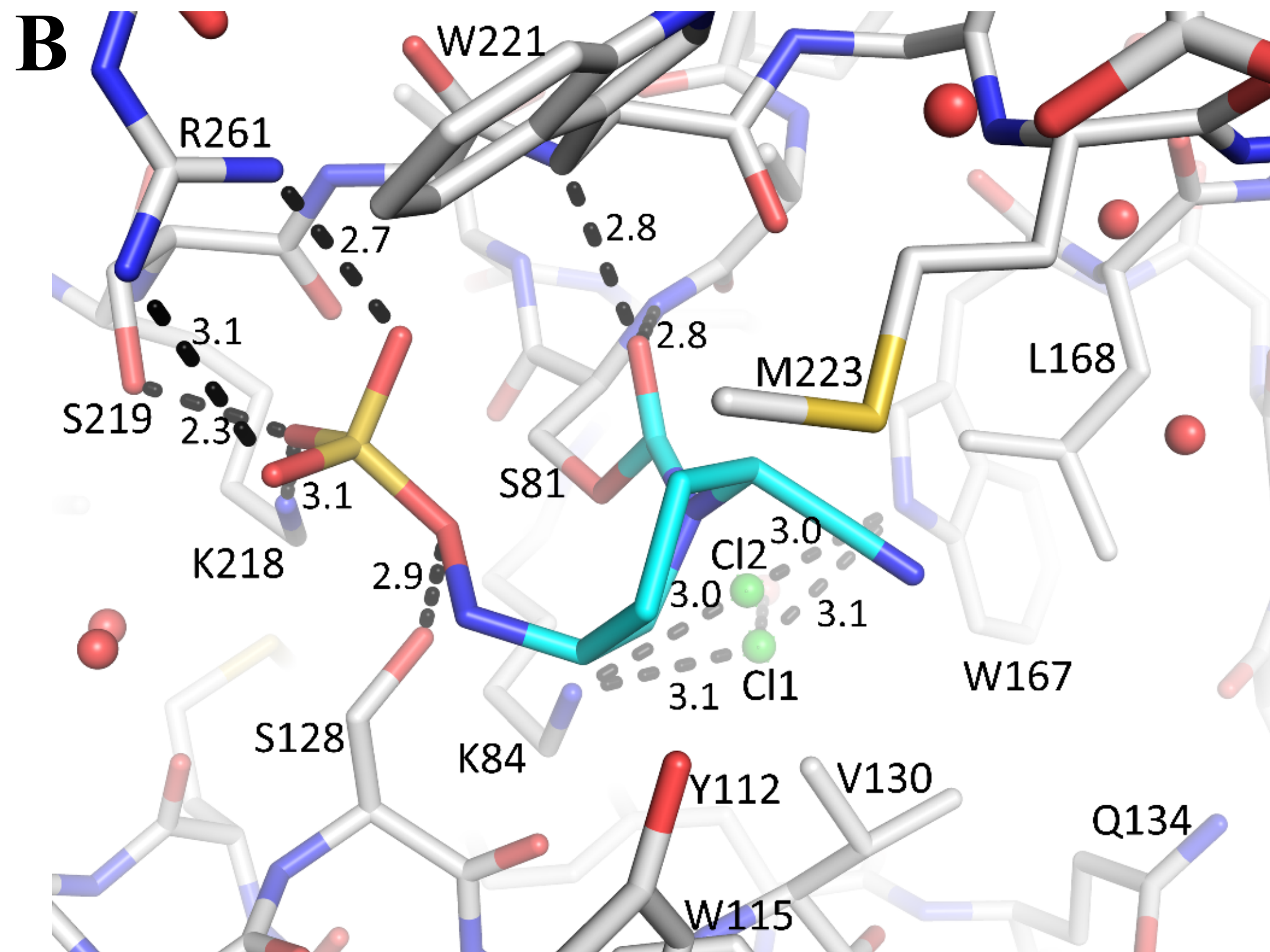
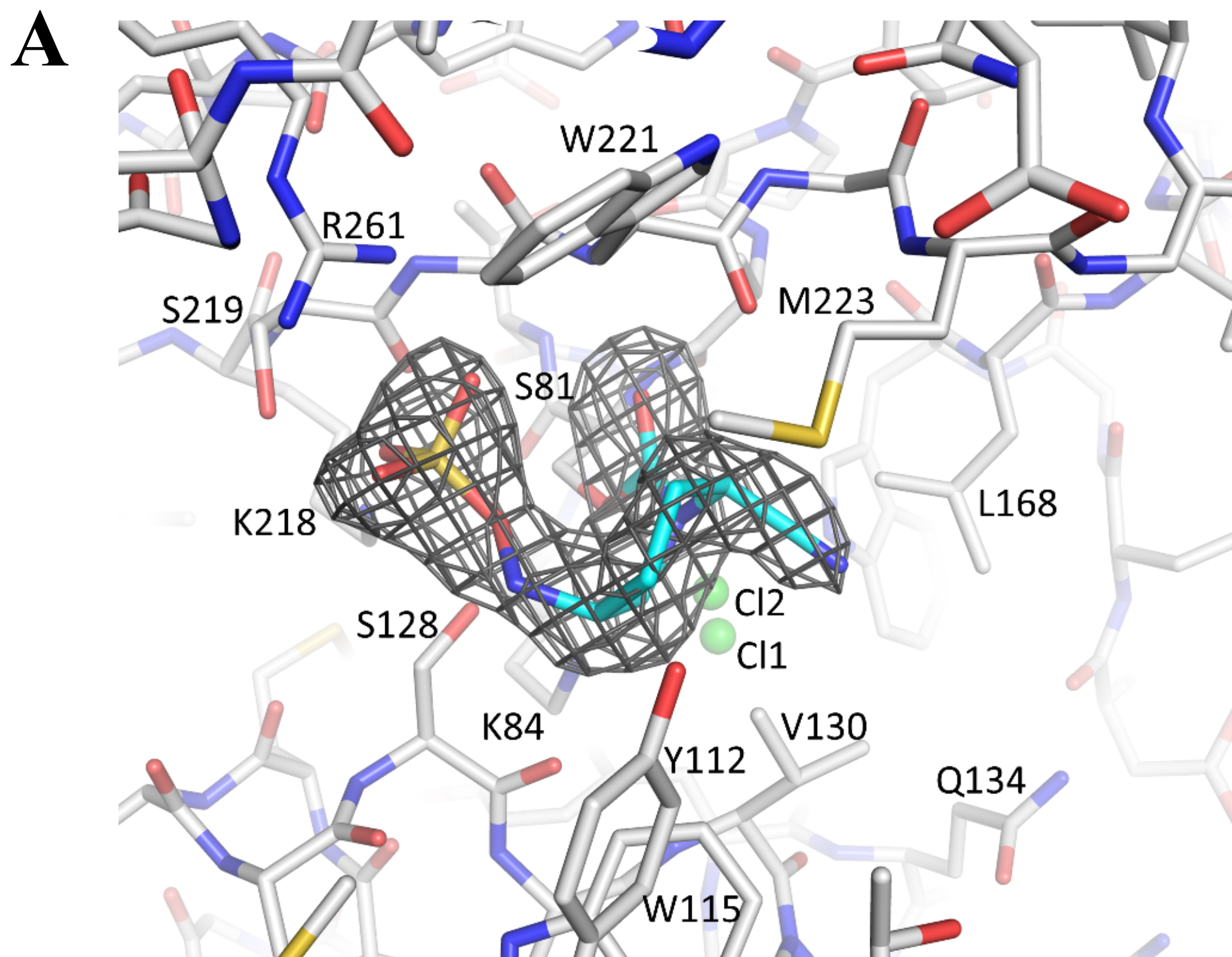
5 min



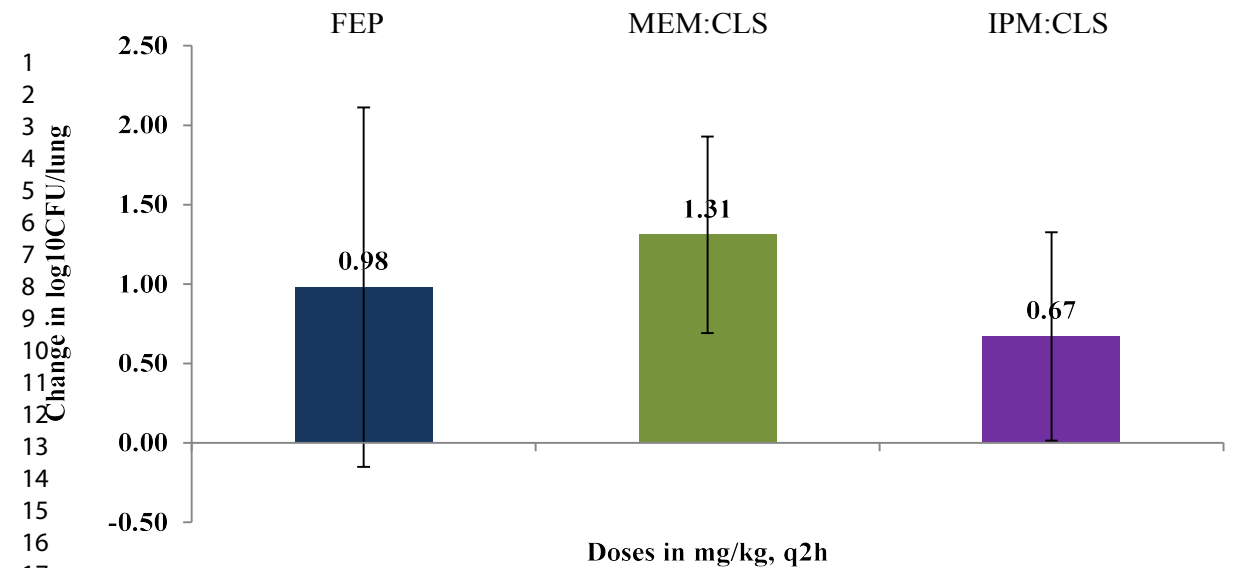
1
2
3
4
5
6
7
8
9
10
11
12
13
14
15
16
17
18
19
20
21
22
23
24
25
26
27
28
29
30
31
32
33
34
35
36
37
38
39
40
41
42
43
44
45
46
47

1
2
3
4
5
6
7
8
9
10
11
12
13
14
15
16
17
18
19
20
21
22
23
24
25
26
27
28
29
30
31
32
33
34
35
36
37
38
39
40
41
42
43
44
45
46
47





A.



B.

